SSC-233

CORRELATION OF MODEL AND FULL-SCALE RESULTS IN PREDICTING WAVE BENDING MOMENT TRENDS

SHIP STRUCTURE COMMITTEE

1972

SHIP STRUCTURE COMMITTEE

AN INTERAGENCY ADVISORY
COMMITTEE DEDICATED TO IMPROVING
THE STRUCTURE OF SHIPS

MEMBER AGENCIES:

UNITED STATES COAST GUARD
NAVAL SHIP SYSTEMS COMMAND
MILITARY SEALIFT COMMAND
MARITIME ADMINISTRATION
AMERICAN BUREAU OF SHIPPING

ADDRESS CORRESPONDENCE TO:

SECRETARY
SHIP STRUCTURE COMMITTEE
U.S. COAST GUARD HEADQUARTERS
WASHINGTON, D.C. 20591

SR-171
1972

Dear Sir:

A major portion of the effort of the Ship Structure Committee has been devoted to improving capability of predicting the loads which a ship's hull experiences. Several research projects have been sponsored in this area.

The enclosed report resulted from such a study. It deals with the comparison of model and full-scale predictions of long-term wave-induced bending moment trends for two similar cargo ships, and demonstrates both the usefulness and the limitations of model testing in determining ship design criteria.

Sincerely,

W. F. REA, III
Rear Admiral, U. S. Coast Guard
Chairman, Ship Structure Committee

SSC-233

Final Report

on

Project SR-171, "Ship Statistics Analysis"

to the

Ship Structure Committee

CORRELATION OF MODEL AND FULL-SCALE RESULTS IN PREDICTING WAVE BENDING MOMENT TRENDS

by

D. Hoffman, J. Williamson, and E. V. Lewis
Webb Institute of Naval Architecture

With Appendices by

O. J. Karst and E. G. U. Band

under

Department of the Navy
Naval Ship Engineering Center
Contract No. N00024-68-C-5282

U. S. Coast Guard Headquarters
Washington, D. C.
1972

ABSTRACT

Comparison is made between model and full-scale predictions of long-term wave-induced bending moment trends for two ships, the S.S. WOLVERINE STATE and the S.S. CALIFORNIA BEAR.

For predicting such statistical trends of wave bending moment from model tests two basic types of required data are discussed:

a. Wave data from different levels of sea severity, along with relationships between wave heights and wind speeds.

b. Model response amplitude operators as a function of ship loading condition, speed and heading.

Available wave data in different ocean areas are first reviewed. The determination of the wave bending moment responses, and the expansion to full-scale are then shown and discussed.

Comparison of predicted long-term trends with extrapolated full-scale results shows good agreement for the WOLVERINE STATE in the North Atlantic and fair results for the CALIFORNIA BEAR in the North Pacific. The inferiority of the latter is probably due to less refined definition of the sea in this ocean area.

It is concluded that success in using the prediction method presented is a function of the quality of sea data available for the particular service in question.

CONTENTS

LIST OF FIGURES

APPENDIX A

SHIP STRUCTURE COMMITTEE

The SHIP STRUCTURE COMMITTEE is constituted to prosecute a research program to improve the hull structures of ships by an extension of knowledge pertaining to design, materials and methods of fabrication.

RADM W. F. Rea, III, USCG, Chairman
Chief, Office of Merchant Marine Safety
U. S. Coast Guard Headquarters

Capt. J. E. Rasmussen, USN
Head, Ship Systems Engineering and Design Department
Naval Ship Engineering Center
Naval Ship Systems Command

Mr. K. Morland, Vice President
American Bureau of Shipping

Mr. E. S. Dillon
Chief
Office of Ship Construction
Maritime Administration

Capt. L. L. Jackson, USN
Maintenance and Repair Officer
Military Sealift Command

SHIP STRUCTURE SUBCOMMITTEE

The SHIP STRUCTURE SUBCOMMITTEE acts for the Ship Structure Committee on technical matters by providing technical coordination for the determination of goals and objectives of the program, and by evaluating and interpreting the results in terms of ship structural design, construction and operation.

NAVAL SHIP ENGINEERING CENTER

Mr. P. M. Palermo - Chairman
Mr. J. B. O'Brien - Contract Administrator
Mr. G. Sorkin - Member
Mr. H. S. Sayre - Alternate
Mr. I. Fioriti - Alternate

U. S. COAST GUARD

LCDR C. S. Loosmore, USCG - Secretary
CAPT C. R. Thompson, USCG - Member
CDR J. W. Kime, USCG - Alternate
CDR J. L. Coburn, USCG - Alternate

MARITIME ADMINISTRATION

Mr. F. Dashnaw - Member
Mr. A. Maillar - Member
Mr. R. Falls - Alternate
Mr. R. F. Coombs - Alternate

MILITARY SEALIFT COMMAND

Mr. R. R. Askren - Member
LTJG E. T. Powers, USNR - Member

AMERICAN BUREAU OF SHIPPING

Mr. S. G. Stiansen - Member
Mr. F. J. Crum - Member

OFFICE OF NAVAL RESEARCH

Mr. J. M. Crowley - Member
Dr. W. G. Rauch - Alternate

NAVAL SHIP RESEARCH & DEVELOPMENT CENTER

Mr. A. B. Stavovy - Alternate

NATIONAL ACADEMY OF SCIENCES - Ship Research Committee

Mr. R. W. Rumke, Liaison
Prof. R. A. Yagle, Liaison

SOCIETY OF NAVAL ARCHITECTS & MARINE ENGINEERS

Mr. T. M. Buermann, Liaison

BRITISH NAVY STAFF

Dr. V. Flint, Liaison
CDR P. H. H. Ablett, RCNC, Liaison

WELDING RESEARCH COUNCIL

Mr. K. H. Koopman, Liaison
Mr. C. Larson, Liaison

INTRODUCTION

A previous report under the current project (1)* dealt with the analysis of ship stress data and the extrapolation of long-term statistical trends. It showed several techniques can be applied to this problem and indicated that a sound basis for predicting loads on similar future ships can be derived. Another report now in preparation (2) attempts to compare and evaluate these extrapolation techniques and to reach definite conclusions.

Meanwhile, however, it has been recognized that the above techniques cannot provide a basis for the design of ships of different or unusual type for which statistical stress data are not available. As pointed out in an earlier paper (3), a proven method of predicting long-term trends from model test results and ocean wave data would be of great value in establishing standards for new ship designs. Such a procedure has been presented (4), and predicted trends for the Wolverine State were shown to agree quite well with the analysis of full-scale stress data (3).

The use of model tests to predict the behavior of ships in a seaway is not new to the naval architect. Ship resistance, propulsion, motions and other parameters can be evaluated in a towing tank by simulating the relevant conditions. However, the comparison of full-scale performance under real sea conditions with simulated model results requires either elaborate instrumentation for full-scale trials or, alternatively, a lengthy procedure of statistical data collection and reduction. The principal approach used in the present project is to make comparisons on a statistical basis, although some limited direct comparisons were made in cases in which wave records were obtained. See Appendix C.

It is helpful here to refer to Fig. 1 from (1), a plot of full-scale ship stress data, which can be interpreted in terms of bending moment, in relation to sea severity -- as grossly measured by wind velocity or Beaufort No. Each dot represents the rms peak-to-trough stress in a 20-minute sample record taken every four hours, i.e., a short-term record that is assumed to be representative of a four-hour interval; a fair curve can be drawn through the average rms values. The first step in the prediction of long-term trends from model results is to predict such an average curve. Another part of the prediction problem is to estimate the standard deviation of these estimated rms values.

As pointed out in (3), a ship in service encounters many different sea conditions in any one voyage, and many more in a year of operation. If we are to predict a long-term bending moment distribution, we need to determine the ship response to many different sea conditions. Hence, we must obtain average or typical spectra representing sea conditions of

*Numbers in parentheses refer to references listed at the end of this report.

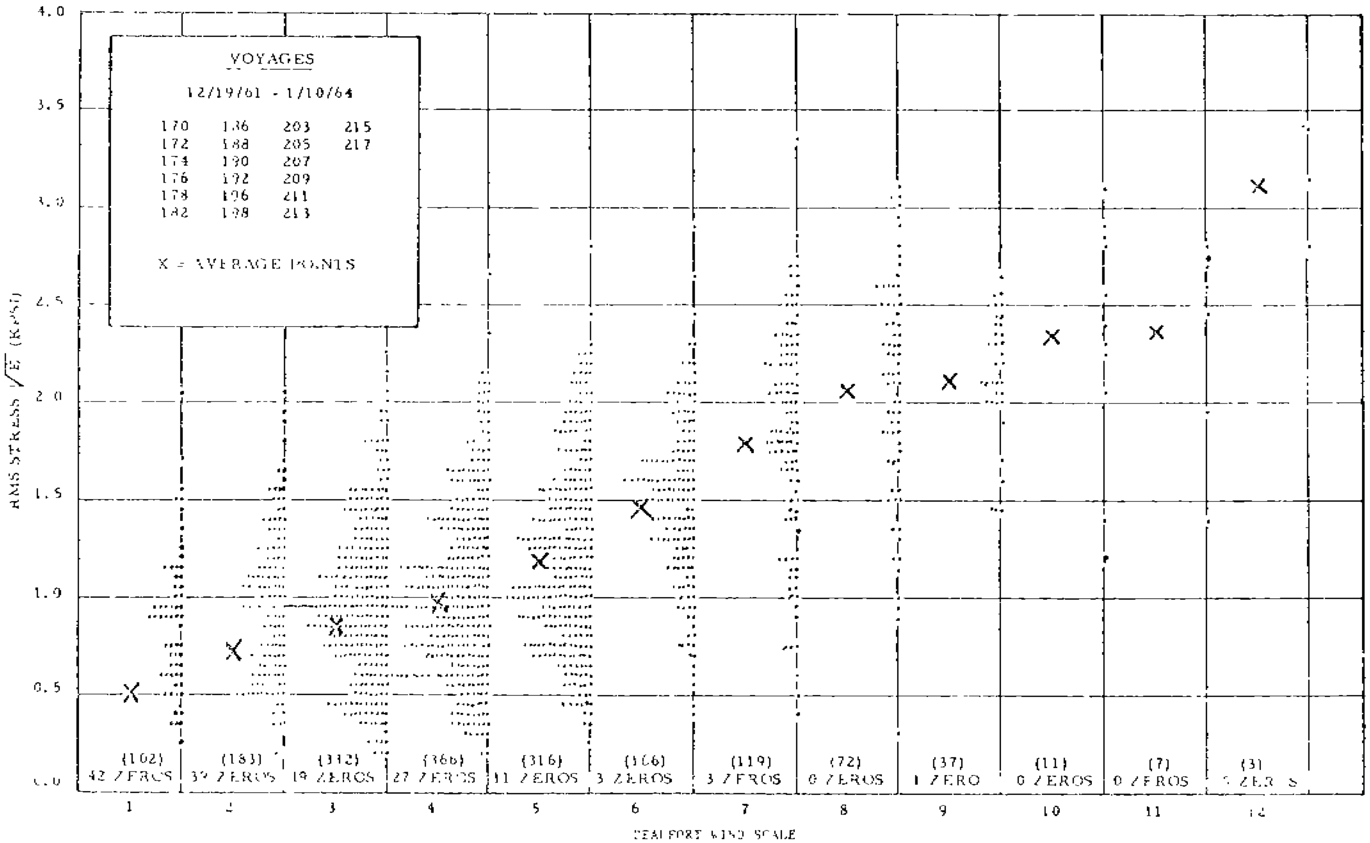

Fig. 1. Typical Plot of r.m.s. Stress Values from Short-Term Records vs. Beaufort Wind Scale for 20 Voyages of S. S. WOLVERINE STATE. (1)

different levels of severity. A spectrum describes the sea by defining the many regular wave components that combine to form the visible wave pattern.

The response of a ship to an irregular sea is described by its response spectrum, which can be predicted by a technique presented some years ago by St. Denis and Pierson (5). This method has been confirmed experimentally (6) and has proved to be very versatile. It involves the assumption that a ship's response to a seaway can be obtained by the linear superposition of its responses to all of the wave components. Using model test results in regular waves, together with the appropriate sea spectrum, this leads to a response spectrum that provides a complete description in statistical terms of the ship's response to that particular sea. Thus the bending moment response can be determined by calculation for any number of representative sea conditions. Computational procedures have been developed at Webb Institute and elsewhere for the determination of wave-induced bending moment at any speed, heading or ship loading for which regular wave model test data are available and for which the sea spectrum is known.

To estimate the standard deviation of bending moment in any given level of sea severity, it is necessary to extend the response calculations to obtain response spectra over a range of sea spectra, all having the same significant wave height. Finally, knowing the relative frequency of occurrence of each sea condition, the weighted long-term bending moment probability distribution can then be obtained, as described later in this report.

For purposes of prediction from model results it is more satisfactory to use wave height than wind speed as a basis for classifying sea spectra, although full-scale data are often referred to wind (Fig. 1). It has been found that a normal distribution of rms bending moment is still applicable, but the standard deviation will be less than when wind is used as a basis (4). In Appendix A it is shown how a prediction of average and standard deviation of rms bending moment vs. significant wave height can be transformed to bending moment vs. wind speed if desired for comparison with full-scale.

It is the purpose of this report to describe in greater detail the technique of predicting long-term trends from model test response data in regular waves and to present a comparison with full-scale data for two different ships on different routes: the S.S. Wolverine State in the North Atlantic, as previously reported (3), and the S.S. California Bear in the North Pacific.

The basic information required for the prediction of statistical trends of wave bending moment is:

1. Wave data for different levels of sea severity, along with relationships between wave and wind data.

2. Response Amplitude Operators for wave-induced bending moment, as a function of ship loading condition, ship speed and ship heading.

Each of these items will be discussed in turn, after which results for the two ships will be presented.

WAVE DATA

Description of the Sea

Experience gained in analyzing short-term records (20 min.) indicates that the statistical behavior of the surface of the sea can be regarded as a Gaussian stationary random process. The sea can be described as a sum of a large number of linearly superimposed elementary sine waves of different frequencies, amplitudes and directions, with random phase angles (5). A typical spectrum is a plot of wave energy $S_\zeta(\omega)$ against wave frequency, ω. It gives an indication of the relative importance (or squared amplitude) of all of the many wave components present in the seaway. Thus one spectrum is sufficient to describe the statistical characteristics of the sea at any one point and time. Since actual sea spectra have a variety of shapes, it is difficult to describe them by simple formulas. However, the use of a spectral family in equation form will be discussed later on.

Another important property of a sea spectrum is that it defines important visible characteristics of the seaway. "Significant wave height" means the average of the one-third highest crest-to-trough wave heights in a record. The average apparent wave period T_1 is defined as the average of the time between successive wave crests, and the average zero-crossing period $\bar{T}$ as the average of the time between successive zero up-crossings. Assuming a sufficiently narrow spectrum, it can be shown (5) that a Rayleigh distribution applies to wave heights, and the significant height, $H_{1/3}$, the average apparent period T_1, and the average zero-crossing period $\bar{T}$ are all functions of the area and moments of the spectrum. Thus,

$$H_{1/3} = 4\sqrt{m_o}$$

$$\bar{T} = 2\pi\sqrt{m_o/m_2}$$

$$T_1 = 2\pi\sqrt{m_2/m_4}$$

where m_o is the area under the spectrum. The moments, m_1 and m_2, can be defined generally in terms of the nth moment m_n of the spectrum as follows:

$$m_n = \int_o^\infty \omega^n \; S_\zeta \; (\omega) \; d\omega$$

It should be noted that, regardless of the applicability of a Rayleigh distribution to peak-to-trough wave heights, the variance σ^2 of the wave surface (sum of the squares of equally spaced points on a record) is also equal to the area m_o under the spectrum. Hence, in the Rayleigh case,

$$H_{1/3} = 4\sqrt{m_o} = 4\sigma$$

where σ is the standard deviation (square root of variance) of the record.

The assumed Rayleigh distribution for the crest-to-trough heights, H, of a short-term wave record can be conveniently expressed in terms of significant wave height, $H_{1/3}$. Thus:

$$P(H) = 1 - \mathrm{Exp}\left[-2 \left(\frac{H}{H_{1/3}}\right)^2\right]$$

As previously noted, "short term" means a period of time which is short enough so that the sea can be described as a stationary, random process, i.e., its statistical properties remain unchanged.

On the basis of the assumed narrow-band process, it can be shown on the basis of (7) that the highest expected value of H in N cycles is:

$$H_{max} = H_{1/3} \sqrt{(\ln N)/8}$$

where ln N is the natural logarithm of N (or $\log_e N$).

After considerable investigation at Webb Institute some time ago, it was decided that for certain types of calculations the "log-slope" spectrum form should be applied, particularly for the response calculations of geometrically similar ships. The log-slope form of spectrum can be obtained as follows:

$$S'_{\zeta}(\log_e \omega) = \frac{S_{\zeta}(\log_e \omega)}{(L_W^2/2\pi)^2} = \frac{2\omega^4}{g^2} \quad S_{\zeta}(\log_e \omega) = \frac{2\omega^5}{g^2} S_{\zeta}(\omega) \qquad [1]$$

where $S'_{\zeta}(\log_e \omega)$ is the log-slope spectrum ordinate (non-dimensional),

$S_{\zeta}(\log_e \omega)$ is an energy spectrum ordinate when plotted against $\log_e \omega$,

$S_{\zeta}(\omega)$ is an energy spectrum ordinate when plotted against ω, ft.^{2}-sec.,

ω is the circular frequency expressed in radians,

L_W is wave length, ft.

Further explanation is given in standard references (8).

In order to convert published spectra given in (9) to this form the following relationships apply:

$$\frac{S'_{\zeta}(\log_e \omega)}{(L_W/2\pi)^2} = \frac{\omega^5}{g^2} \times \frac{180}{\pi} \text{ CORR. FT.}^2$$

where (CORR. FT.^{2}) = Spectral ordinate of (9) = $\frac{2\pi H}{180}$, where H is the "lag number" i.e., spectral abscissa.

Table I gives the values of ω, T and L_W corresponding to different values of $\log_e \omega$.

Table I. Wave Length L_W, for Given Values of $\text{Log}_e\ \omega$

$\log_e \omega$	ω 1/sec.	T sec.	T^2 $(sec.)^2$	L_W feet
0.2	1.2215	5.144	26.461	135.6
0.1	1.1052	5.685	32.319	165.6
0	1.0000	6.283	39.476	202.2
-.1	.9041	6.950	48.302	247.4
-.2	.8189	7.673	58.875	301.6
-.3	.7408	8.482	71.944	368.6
-.4	.6703	9.374	87.872	450.1
-.5	.6065	10.360	107.33	549.9
-.6	.5488	11.449	131.08	670.2
-.7	.4966	12.652	160.07	820.0
-.8	.4493	13.984	195.55	1001.8
-.9	.4066	15.453	238.80	1223.4
-1.0	.3679	17.078	291.66	1494.2
-1.1	.3329	18.874	356.23	1825.0
-1.2	.3012	20.860	435.14	2229.2
-1.3	.2725	23.058	531.67	2723.7
-1.4	.2466	25.479	649.18	3325.7
-1.5	.2231	28.163	793.15	4063.3
-1.6	.2019	31.120	986.45	4961.4

$\omega = 2\pi f = \frac{2\pi}{T}$ $\qquad L_W = \frac{gT^2}{2\pi} = 5.123\ T^2$

Information regarding ocean waves and winds at various localities around the world is rather spotty. The North Atlantic Ocean, due to its importance as a trade route and its reputation for severe storms, has been the subject of more extensive investigation than any other region. It was therefore possible to make use of spectra obtained from actual wave records in the North Atlantic on which to superimpose model data in the case of the Wolverine State (3).

However, wave information regarding the North Pacific is limited to visual observations of wave heights and periods. In order to predict the performance of a ship in the Pacific it is therefore necessary to make use of spectral formulations selected to match the observed data. Both approaches were tried in this study for the Wolverine State in the North Atlantic, since it was assumed that, if correlation between the two methods was satisfactory there, the observed wave data for the North Pacific could then be used for predicting trends in that ocean.

Compilations of Spectra

The most desirable form of wave data is collected spectra obtained from actual wave records. The best collection of spectra is that derived at New York University (9) from records obtained by the National Institute of Oceanography (Great Britain) from wave records taken on weather ships in the North Atlantic. To predict a ship's response to the wide range of conditions to be found at sea, it is convenient to classify or subdivide sea spectra into several contiguous ranges of significant wave height ($H_{1/3}$).

A typical family of six curves obtained from New York University data (9) is shown in Fig. 2. From the total population of 460 spectra, 10 sample spectra were randomly chosen for each of four groups having significant wave heights of 10, 20, 30, and 40 ± 5 feet. The ten sample spectra having the 30-foot significant wave height are shown in Fig. 3 in log-slope form, a form that was described previously.

In addition, a number of very severe sea records were obtained from the National Institute of Oceanography (Great Britain) and were analyzed by Pierson. From these the 12 most severe were used to obtain a fifth group to supplement the above four. The average significant wave height of these severe spectra was 48.2 feet. Thus a total of five groups classified by average significant wave height was obtained based on an actual sample of 52 spectra. Figure 4 shows the complete family of average sea spectra in log-slope form (3).

For applications of probability theory we need more than typical average spectra; we need information on their variability. This is provided by using all the individual spectra randomly selected to obtain the average (such as Fig. 3). It will be shown later that the standard deviation of bending moment in each sea condition can be determined by calculation of bending moment response to <u>all</u> the spectra corresponding to that wave height.

Observed Wave Data

The second form in which ocean wave data are available is in tabulations giving the frequency of occurrence of different combinations of H_V and T_V values for different ocean areas, where H_V and T_V are the visual average wave height and period, in ft. and sec., respectively. A most comprehensive collection of such data is given in (10), where data for 50 ocean areas are tabulated for different seasons and different wave directions for a range of wave periods varying roughly from 6.0 sec. to 22.5 sec. over ten increments. Data are based on almost two million sets of observations reported from ships at sea over a period of eight years. The reports are estimates of wave characteristics as seen by untrained observers on board. The data are subdivided into three monthly periods representing the typical four seasons for each defined zone.

Unfortunately, data are not given in (10) for the North Pacific. However, limited Pacific data are given by the ISSC (11) and more extensive data by Yamanouchi (12). In these sources three tables are given for each zone: i.e., period vs height, direction vs. height and direction vs period. This form of tabulation is essentially "open ended,"

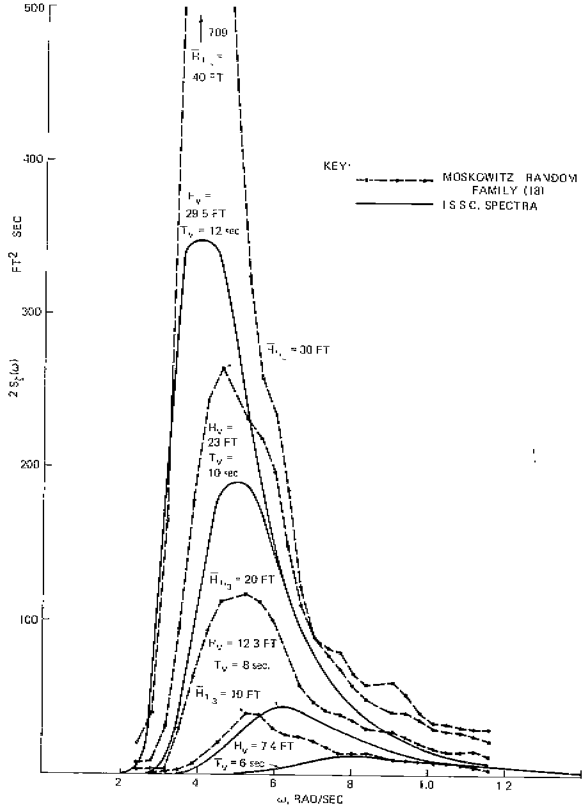

Fig. 2. Comparison of Moskowitz and ISSC Spectra

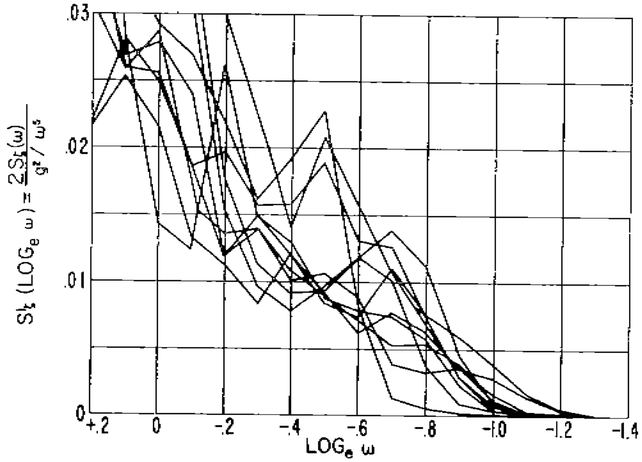

Fig. 3. Sample of the Ten Wave Spectra Used to Obtain the 30-ft. Significant Wave Height Spectrum

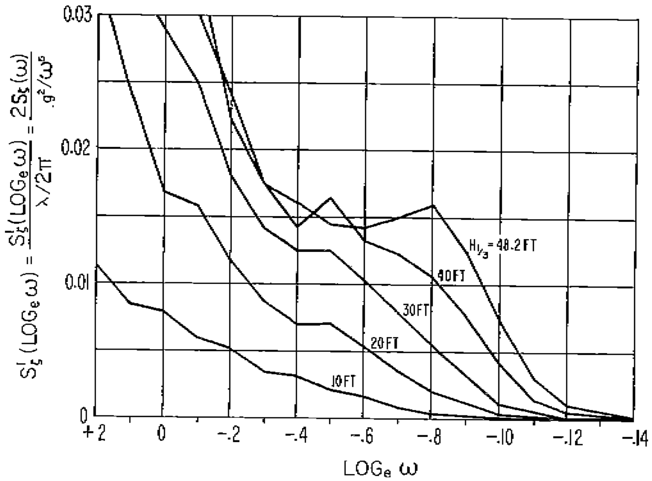

Fig. 4. Family of Sea Spectra Based on Wave Height

i.e. for the highest category the average values of H_V and T_V can only be estimated at the user's discretion.

Table II illustrates a typical summary for one sea zone (North Pacific) as given by Yamanouchi (12), averaged over all directions for an entire year. Fig. 5 gives two histograms of wave heights based on ISSC data (11) for Area 18 in the North Atlantic and Area 3 in the North Pacific, covering all wave directions and periods for a year. Reasonably good agreement between these oceans is shown.

In order to use such data for our purpose, it is necessary to select suitable spectra to correspond to the tabulated values of H_V and T_V. The spectrum formulation most generally used is in the general form presented by Pierson (13):

$$S_\zeta(\omega) = \frac{A}{\omega^5} \operatorname{Exp}\left(-\frac{B}{\omega^4}\right) \qquad [2]$$

where $S_\zeta(\omega)$ is the energy spectrum ordinate, ω the wave frequency, and A and B are constants.

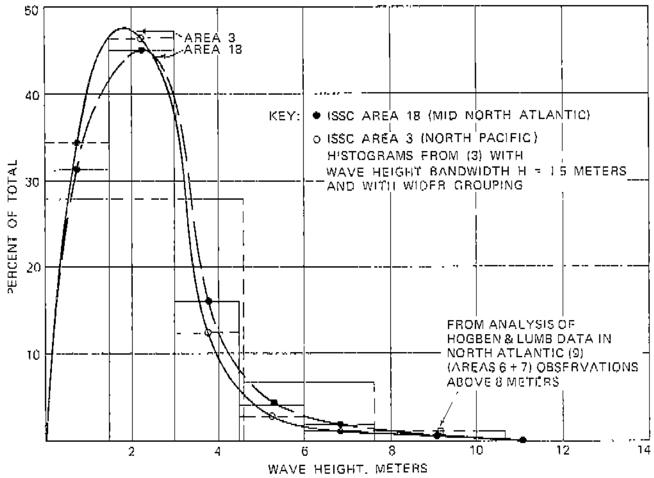

Fig. 5. Histograms of Wave Heights for All Year, All Directions, All Periods on North Atlantic Compared to ISSC Data

Table II. Typical North Pacific Wave Data (12) in Terms of Frequency of Occurrence, %

Wave Height vs Wave Period
No. of Observations = 100,894

H_V ft.	T, sec. T < 5	5<T<7	7<T<9	9<T<11	11<T<13	13<T<15	15<T	Calm	Total
0 < H < 4.1	28.21	9.27	1.93	0.29	0.11	0.03	2.12	0	40.98
4.1< H < 9.0	6.92	17.87	13.85	4.82	0.86	0.16	0.09	0.	44.57
9.0< H < 13.8	0.35	1.47	2.86	2.89	1.86	0.67	0.14	0.	10.24
13.8< H <18.9	0.07	0.19	0.33	0.39	0.19	0.10	0.10	0.	1.42
18.9< H <25.4	0.02	0.08	0.22	0.24	0.25	0.14	0.06	0.	1.01
25.4< H	0.	0.02	0.06	0.08	0.10	0.08	0.06	0.	0.40
Calm	0.	0	0.	0.	0.	0.	0.	1.38	1.38
Total	35.57	27.90	19.37	8.71	1.37	1.16	2.57	1.38	100.00

The 11th ITTC recommended as an interim standard a formulation based on equation [2] in which $A = 8.1 \times 10^3 g^2$ and $B = 33.56/H^2_{1/3}$, the single parameter being significant wave height, $H_{1/3}$.

It can be shown that for the above values of A and B, the average period (from zero crossings) is,

$$\bar{T} = 1.96\, H_{1/3}$$

Thus not only is the shape of any spectrum fixed but also the relationship between the significant wave height and the average period. Hence, this simple one-parameter formulation is not satisfactory here, although it can be used for other purposes.

A form of the Pierson-Moskowitz spectrum involving the two-parameters $H_{1/3}$ and average period is more suitable for our purpose, and several such formulations have been proposed by various writers, usually expressed in non-dimensional form. The formulation adopted here is that derived by the ISSC (11) from Equation [2]. It was assumed that $H_V = H_{1/3}$ and $1/T_V$ is equated to the first moment of the spectrum.

$$S_\zeta(\omega) = \frac{.11\, H_V^2}{T_V^4 \left(\omega/2\pi\right)^5}\ \mathrm{Exp}\left\{-\frac{0.44}{T_V^4 \left(\omega/2\pi\right)^4}\right\} \qquad [3]$$

where $S_\zeta(\omega)$ is the energy spectrum ordinate in ft.^{2}-sec.

It may be seen that a single spectrum can be selected to correspond to any given values of H_V and T_V. (Some studies suggest that the relationships are not really so simple). A typical family of six curves is given in Fig. 6 in the form $S_\zeta(\omega)/H_V^2$. Since the spectral ordinate is proportional to H_V^2, the curves at different periods (one for each T_V) represent an array of infinite number of spectra depending on the number of wave height groups selected.

Alternatively, the ISSC spectra in "log-slope" form are given in Fig. 7, where a spectral ordinate is given by $S_\zeta(\log_e \omega)/H_V^2$, and,

$$S_\zeta(\log_e \omega) = \frac{2\, S_\zeta \log_e(\omega)}{\left(\omega/2\pi\right)^2} = \frac{342.9\, H_V^2}{g^2\, T_V^4}\ \mathrm{Exp}\ -\left\{\frac{686}{T_V^4\, \omega^4}\right\} \qquad [4]$$

The abscissa of Fig. 7 is $\log_e \omega$.

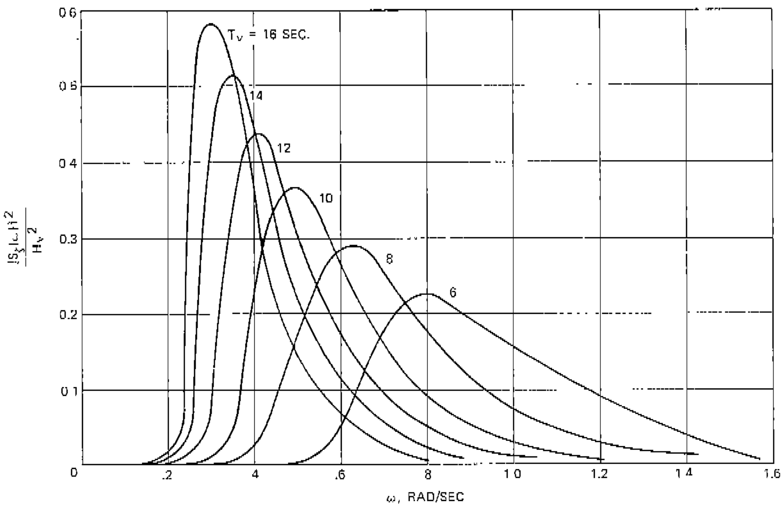

Fig. 6. ISSC Sea Spectrum Family

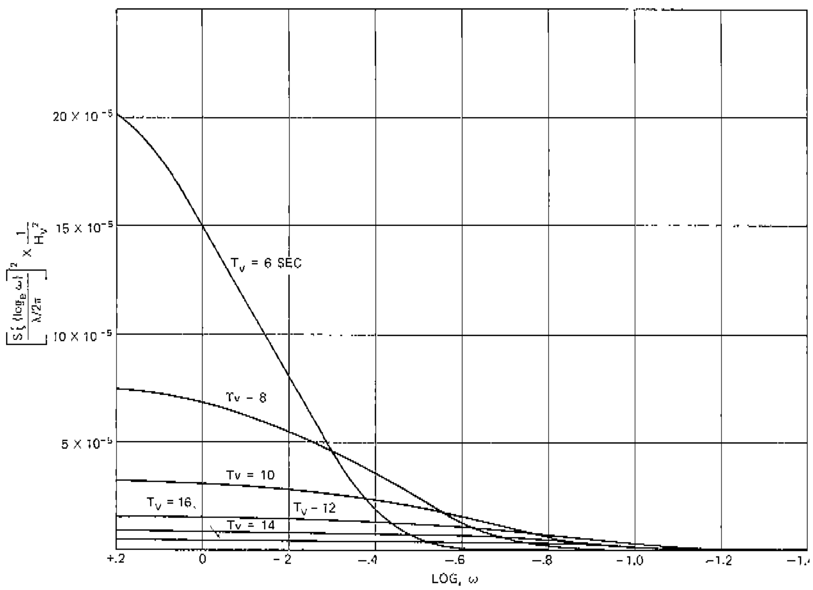

Fig. 7. ISSC Sea Spectrum Family in Log-Slope Form

It may be noted that some aspects of ship performance at sea -- such as motion amplitudes, added power, or probability of shipping water -- can be predicted more simply than a long-term distribution of bending moment. It is customary in such cases to define a number of different sea conditions by using a spectrum formulation such as [2]. After ship responses are calculated in each spectrum, a weighting function can be applied giving the assumed percentage of time that each condition will occur in service. Hence, average performance can be predicted for typical service conditions. However, since such a procedure does not consider the scatter of response in each sea condition (i.e. standard deviation) it does not permit the prediction of the probability of exceeding high values of quantities such as bending moment.

Short-crestedness

The sea spectra given in publications such as (8) are point spectra and represent irregular seas as observed at a fixed point with no indication of the spread in direction of the component waves. However, for reliable predictions of bending moments from model data, it has been found (14) that the short-crestedness of actual ocean wave patterns resulting from the different directions of the various components must be taken into account. British wave buoy records (15) confirm an earlier stereo photographic study (16) in indicating that an angular distribution of wave energy proportional to the square of the cosine of the angle between the component wave and the dominant wave direction is a good approximation. Hence, the short-crested spectrum can be obtained by multiplying the point spectrum by a spreading function

$\frac{2}{\pi}\cos^2 \mu_W$, where μ_W is the direction of a wave component relative to the direction of the wind. It has been suggested that the exponent of the cosine should have some other value than 2, and that the value should vary with frequency. A general formulation was most recently recommended by the 12th ITTC of the spectrum with spreading function:

$$S_\zeta(\omega, \mu_W) = \frac{k}{\pi} \cos^n \mu_W \, S_\zeta(\omega)$$

$$-\frac{\pi}{2} < \mu_W < \frac{\pi}{2}$$

However, at present there is believed to be insufficient evidence to justify departing from the simple cosine squared relationship. Hence,

$$S_\zeta(\log_e \omega, \mu_W) = \frac{2}{\pi} \cos^2 \mu_W \, S_\zeta(\log_e \omega) \qquad [5]$$

The total energy in all components of the directional spectrum is the same as the total energy in the point spectrum because

$$\int_{-\frac{\pi}{2}}^{+\frac{\pi}{2}} \frac{2}{\pi} \cos^2 \mu_W \, d\mu_W = 1$$

Wave Height Vs. Wind Speed Relationship

As previously noted, predictions of bending moment from model tests can best be based on wave height as the sea state parameter, whereas full-scale data are usually classified by Beaufort number. Hence, a relationship between wind speed and wave height must be determined.

Several relationships between wave height and wind speed are commonly given for open ocean conditions. However, care must be taken to distinguish those representing ideal fully developed seas from those describing average conditions. Fig. 8 shows relationships derived from various sources.

The steepest line, though not necessarily the highest in the low Beaufort No. region, is the Pierson-Moskowitz curve derived for the ideal case of fully-developed seas (13) and therefore not suitable for the present case in which average conditions are sought.

A shallower line was recommended by the 11th ITTC (1966) as an interim standard based upon the "Moskowitz Random" line which was obtained by random sampling of available spectra (17). This line was intended to define typical heights for seas at random stages of partial development and is correspondingly lower than the fully arisen Pierson-Moskowitz line for higher wind speeds. For low wind speeds it lies above the Pierson-Moskowitz line, thus allowing for residual swells which will typically accompany the wind sea. However, Pierson has pointed out that that "population" from which his sampling is made (9) is biased in favor of seas that are near full development and therefore may show wave heights that are somewhat too high. Also shown in Fig. 8 is a curve of standard deviation of wave height in relation to wind, s_3, as obtained from an analysis of spectra (9). It will later be shown that this information is essential in order to relate the standard deviation of the response in relation to wave height to that in relation to wind speed. (Appendix A).

A simpler wind-wave relationship adopted by the British Towing Tank Panel has also been shown in Fig. 8. It is a straight line defined by the formula:

$$H_{1/3} = aU + b \qquad [6]$$

where $H_{1/3}$ is the significant wave height, U is the wind speed in knots and a and b are constants. This relationship can be regarded as a rough approximation of the Moskowitz random line, but it is somewhat lower in both the low and high wind ranges.

Another relationship is that given by Roll (18) on the basis of observed wave heights. There is some doubt, however, whether the "observed wave height" corresponds to the "significant wave height" as used in the previously discussed cases. Furthermore, Roll's curve has to be extrapolated beyond Beaufort 10 due to lack of high sea data. A modified curve has therefore been suggested by Hogben based on his relationship between observed height H_{OBS} and significant height as follows:

$$H_{1/3} = 4.1 + .89\, H_{OBS} \qquad [7]$$

However, the modified Roll curve still seems low compared to other suggested lines. The standard deviation as given by Roll is also shown in Fig. 8.

A recent addition to the family of curves is that given by Scott (19) which closely fits the formula:

$$H_{1/3} = .08U^{3/2} + 5 \qquad [8]$$

He found that this formula fits the Pierson-Moskowitz observations of wave height for winds from 15 to 55 knots with standard error $\sqrt{\frac{s}{n}}$ of 6 ft.

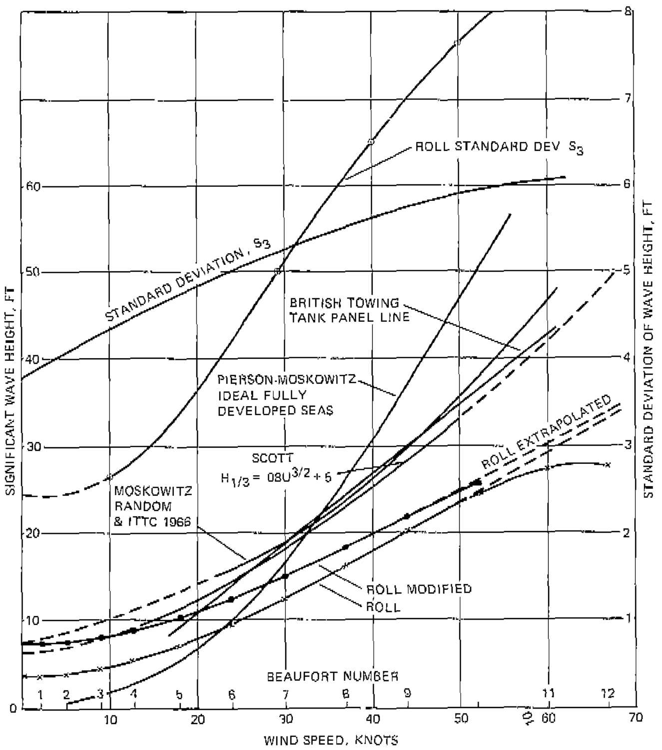

Fig. 8. Relationship between Significant Wave Height and Wind Speed from Various Sources, and Standard Deviation of Wave Height Relative to Wind

Results obtained from the Tucker wave meter on board the Wolverine State for two typical North Atlantic voyages (west and eastbound) are presented in Fig. 4C, Appendix C. The wave height recorded (significant) is plotted against wind speed for a total of 93 twenty-minute records, and the average curve representing this relationship is shown. Also illustrated are values obtained by Roll from observed wave height, corrected to significant wave height using the above Equation [7]. Reasonably good agreement prevails for the range of wave height adequately documented by actual measurements, indicating consistency between Tucker meter results and corrected Roll results.

However, it should be noted that all the above relationships were derived from data collected in the North Atlantic. It is unreasonable to assume that in the North Pacific these relationships are necessarily the same. The only available source of such information regarding the Pacific is Yamanouchi (12). The data are based on 100,000 observations collected from various untrained observers over a period of four years. Fig. 9 illustrates the Yamanouchi wind vs. wave height relationship for the North Pacific and Roll for the North Atlantic redrawn from Fig. 8. The standard deviations are also given for both curves in Fig. 10. The Yamanouchi curve (Fig. 9) was corrected to give significant wave height rather than observed height using Equation [7]. It is readily observed that the Yamanouchi curve is rather low in comparison to Moskowitz and is even lower than Roll's curve which, however, was derived in a similar manner from visual observations.

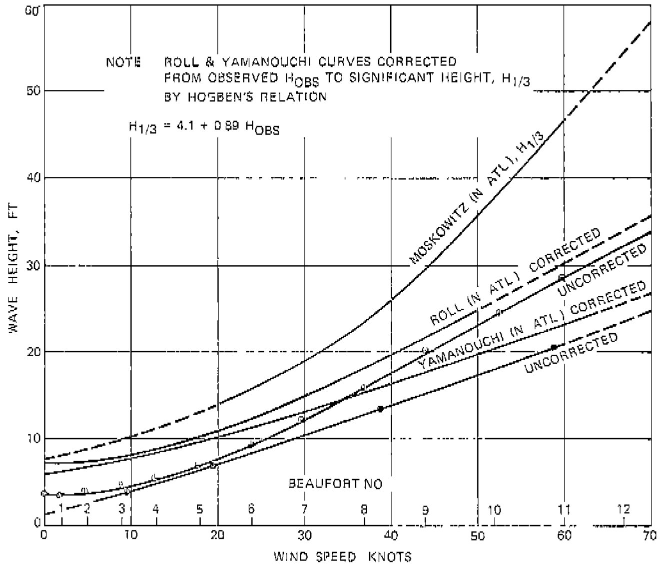

Fig. 9. Relationship Between Significant Wave Height and Wind Speed from Various Sources

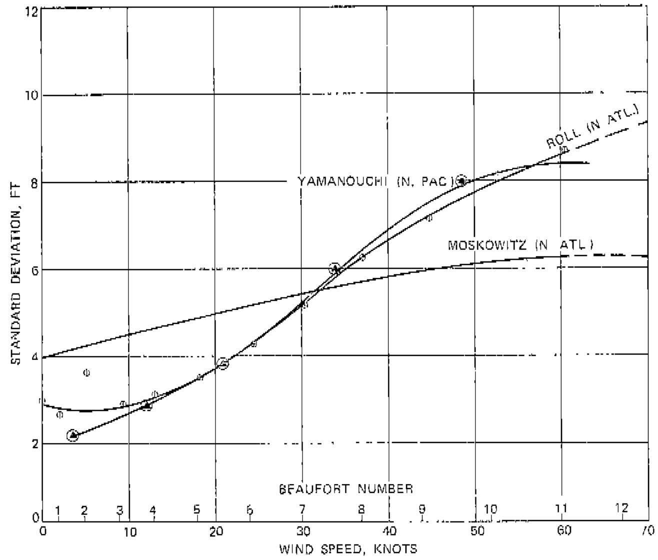

Fig. 10. Wind-Wave Height Standard Deviations from Various Sources

Although the Moskowitz random line was selected for use in the previous analysis (3) there is now reason to believe that the Roll relationship may be more suitable. Detailed comparison between the Yamanouchi and the Roll curves and the standard deviations is given in Table III.

Table III. Wind Speed vs. Wave Height Relationships Derived from Roll (18) and Yamanouchi (12)

Beaufort Numbers	Average Wind Speed, Knots	Significant Wave Height $H_{1/3}$, Feet: Roll N. Atlantic	Significant Wave Height $H_{1/3}$, Feet: Yamanouchi N. Pacific	Standard Deviation Feet: Roll N Atlantic	Standard Deviation Feet: Yamanouchi N. Pacific
1 & 2	3.5	7.4	6.4	2.62	2.00
3 & 4	11.0	8.5	8.1	2.78	2.70
5 & 6	21.0	11.2	10.7	3.67	3.65
7 & 8	33.5	16.6	14.4	5.53	5.65
9 & 10	48.0	23.9	19.0	7.46	7.65
> 10	63.5	33.0	24.3	8.79	8.20

All wave heights are significant values (average of highest one-third), as derived from the observed values given in Refs. (18) and (12) according to Hogben (10) as follows:

$$H_{1/3} = 4.1 + 0.89\ H_{OBS}$$

RESPONSE AMPLITUDE OPERATORS (RAO's)

Experimentally determined R.A.O.'s for the Wolverine State and the California Bear at seven different headings of 0°, 30°, 60°, 90°, 120°, 150° and 180° were obtained from model tests in regular waves at the Davidson Laboratory (20) (21).

These data were presented in plots of M/ζ, Vertical Bending Moment (M) over Wave Amplitude (ζ), against ship speed for a range of L_W/L

ratios, Wave Length (L_W) over Ship Length (L), of 0.2 to 2.0 and speeds of 8-22 knots.

The results for the Wolverine State are given for a mean draft of 19.3 ft., simulating an average load condition of the ship on the North Atlantic route, as well as for the 30 ft. even keel fully loaded condition (not actually attained in service).

The California Bear too was tested at two loading conditions, at mean drafts of 24.625 ft. and 20.9 ft., representing average loading conditions on the westbound and eastbound voyages, respectively, across the North Pacific. Cross plots of M/ζ against L_W (eff)/L were made for ship speeds of 8 and 16 knots for the Wolverine State and 14 and 21 knots for the California Bear, where L_W (eff) = $L_W/\cos\mu_W$, μ_W being the heading angle relative to wave direction. This form of cross plot was adopted because the R.A.O. curves for the various headings should all peak at approximately L_W (eff)/L = 1, and this enables fairing to be more easily accomplished.

The R.A.O.'s were then transposed from M/ζ to a non-dimensional form (7):

$$Y'_{H_e/L_\zeta} = \left[\frac{H_e/L}{2\pi\zeta_a/L_W}\right]^2 = \frac{(M/\zeta)\left\{L_W/L \Big/ 2\pi/L\right\}^2}{c\ \rho\ g\ L^3\ B\ C_W} \qquad [9]$$

where H_e/L is the non-dimensional bending moment coefficient, $2\pi\ \zeta_a/L_W$ is maximum wave slope, and ($c\ \rho\ g\ L^2\ B\ C_W$) is the conventional quasi-static bending moment per unit wave height, with C_W the waterplane coefficient and c a coefficient obtained from Swaan (22).

H_e is the effective wave height, defined as the height of a trochoidal wave whose length is equal to that of the ship, which by conventional static bending moment calculations (Smith effect excluded) gives a bending moment (hog or sag) equal to that experienced by the ship in an irregular sea. Hence, by the above definition,

$$H_e/L = \frac{BM}{2\rho\ g\ L^3\ B\ c\ C_W}$$

In this case, the irregular sea B.M. is the rms peak-to-trough value. It is possible to convert H_e/L to bending moment, or to a non-dimensional coefficient, μ, where

$$\mu = \frac{BM}{2\rho\ g\ B\ L^3} = \left(H_e/L\right)\ c\ C_W$$

The values of c and C_w for the Wolverine State and the California Bear are given below:

	c	C_w	$c\ C_w$
Wolverine State	.01955	.752	.01470
California Bear	.01899	.724	.01375

The R.A.O.'s were plotted against $\log_e \omega$ as shown in Figs. 12-17 for all conditions and two speeds each, where

$$\log_e \omega = \log_e \sqrt{\frac{2\pi\ g/L}{L_{Weff}/L}}$$

$$= \log_e \frac{.61872}{\sqrt{L_{Weff}\ L}} \qquad [10]$$

Since model test results did not cover the very long wave lengths encountered in severe storms at sea, the R.A.O. curves were extrapolated by fairing to the quasi-static values obtained from Swaan (22). The static bending moment M_W as given by Swaan is:

$$M_W = \rho\ g\ \bar{h}\ B\ L^2\ m_W$$

where $\bar{h}$ is wave amplitude and m_W is Swaan's static bending moment coefficient ($2c\ C_W$ in the previous notation). In the case of the California Bear,

m_W = .02716 (22), and hence for $L_W/L = 1.0$ and $2\bar{h} = L/20$,

$$M_W = 216{,}000 \text{ ft.-tons}$$

The corresponding figure obtained from the Davidson Laboratory model tests (21) was 152,000 ft.-tons. The latter result includes effects associated with model motions and forward speed, and therefore, it is lower, as expected. However, the static values obtained from Swaan were very helpful in showing trends for fairing the RAO curves, especially in extrapolating to the longer wave lengths for which no experimental data were available. Fig. 11 shows curves obtained by first calculating static bending moments for the California Bear on the basis of (22) and then applying a dynamic factor. This factor was simply the ratio of model/static bending moment at $L_W/L = 1.5$.

Comparing the R.A.O.'s of the Wolverine State and California Bear it will be noted that the former are much smoother and more regular than the latter. This is partly due to the fact that the Wolverine State data were faired, whereas the California Bear data were not. Since the calculation of ship response is a summing up process, it should make little difference whether input data are faired or not. It should also be noticed that the vertical scale of the California Bear response is given in terms of the

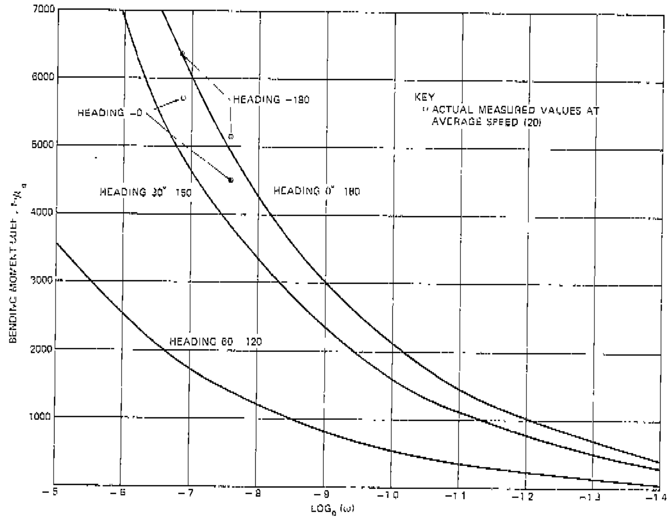

Fig. 11. Adjusted "Swaan Curves" for CALIFORNIA BEAR, - Static Wave Bending Moment

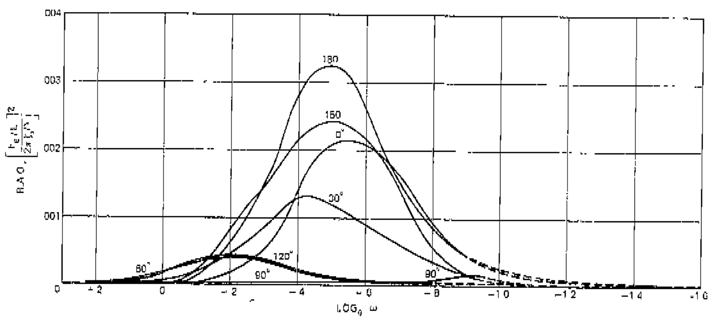

Fig. 12. Bending Moment Response Amplitude. Operators, S.S. WOLVERINE STATE, 8 Knots Speed, from Model Tests (20)

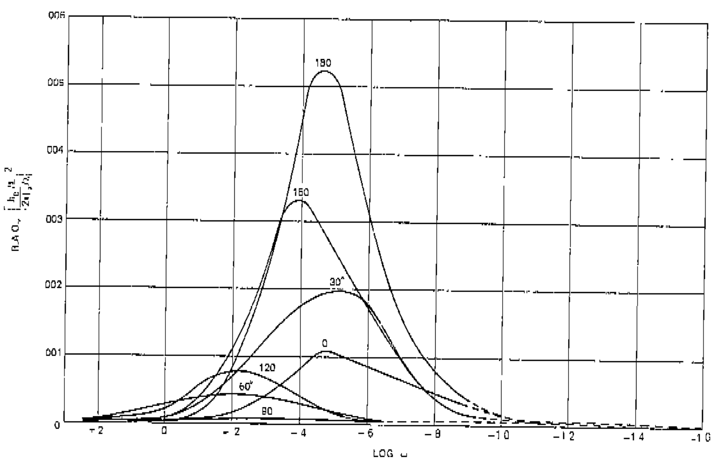

Fig. 13. Bending Moment Response Amplitude Operators, S.S. WOLVERINE STATE, 16 Knots Speed from Model Tests (20)

square of non-dimensional response instead of the first power, as in Figs. 12 and 13 for the Wolverine State. However, a more important difference is that the California Bear model results showed a distinctly two-peaked characteristic not found in the other ship. This may represent simply a difference between the two hulls or be the result of a more thorough set of model tests with more data points in the case of the latter ship. (Double peaked curves are discussed in (23)).

The R.A.O.'s for both ships were then read off the plotted curves (Figs. 12-17) at 19 values of $\log_e \omega$ between the values of +.2 to -1.6 at increments of 0.1 for the seven headings investigated. The 19 values read for each heading constitute the entire model information which was used as input to a computer program, along with wave spectrum data, to give the mean response and its standard deviation at different levels of wave height.

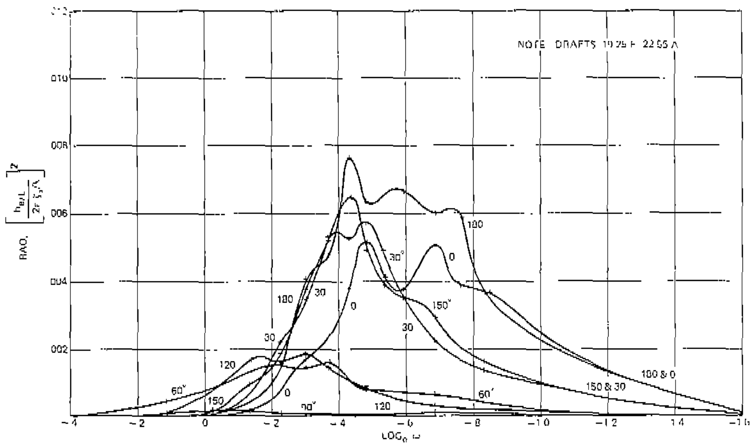

Fig. 14. Bending Moment Response Amplitude Operators, S.S. CALIFORNIA BEAR, 14 Knots Speed, Light Draft from Model Tests (20)

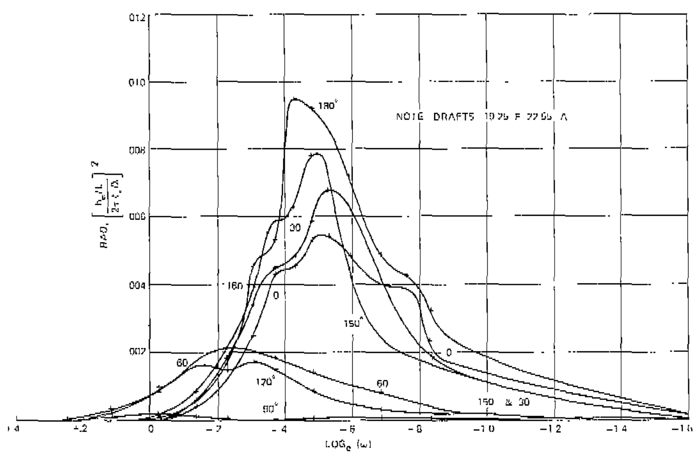

Fig. 15. Bending Moment Response Amplitude Operators, S.S. CALIFORNIA BEAR, 21 Knots Speed, Light Draft from Model Tests (20)

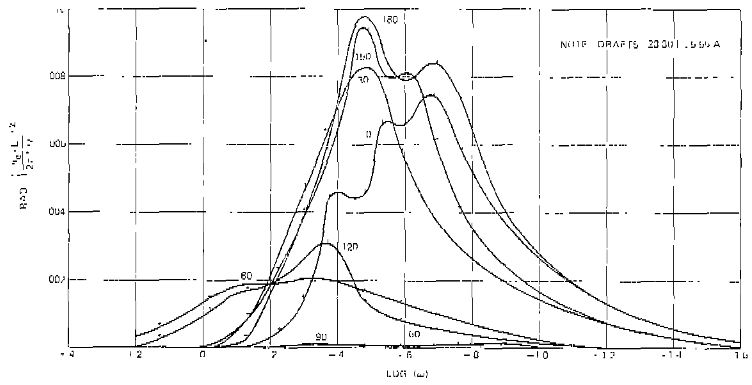

Fig. 16. Bending Moment Response Amplitude Operators, S.S. CALIFORNIA BEAR, 14 Knots Speed, Deep Draft from Model Tests (21)

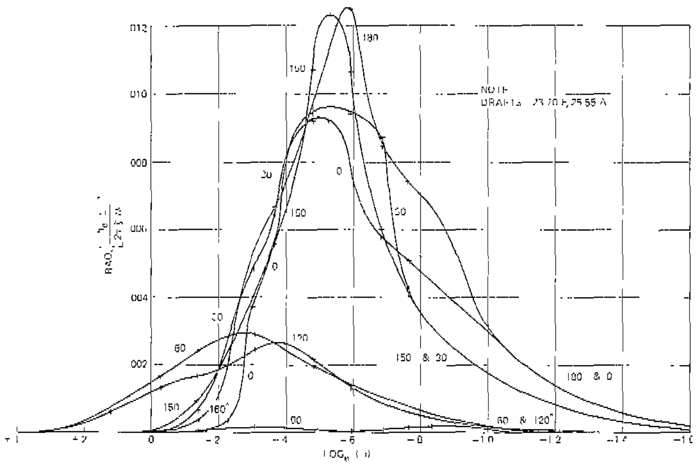

Fig. 17. Bending Moment Response Amplitude Operators, S.S. CALIFORNIA BEAR, 21 Knots Speed, Deep Draft from Model Tests (21)

WAVE BENDING MOMENT RESPONSES - MODEL

The prediction of wave-induced bending moments on ships operating in realistic short-crested irregular seas can now be accomplished by the principle of superposition (26) in which R.A.O.'s from model test results and the short-crested sea spectra discussed above are combined. In each case the products of points on a wave spectrum component curve and the corresponding R.A.O. curve at the same $\log_e \omega$ and the same heading angle give points on the bending moment response spectrum component curve.

Calculations of the response spectrum component curves and the integration of these curves over a spread of $\pm$ 90° from the dominant wave direction, to give the integrated response spectrum curve, were carried out by electronic computer. The response spectrum curves are useful mainly in terms of the areas which they enclose, because these can be interpreted statistically.

Hence, the computer program performs the integrations:

$$R = \int_{\mu} \int_{\omega} \quad S_{\zeta}(\log_e \omega,\ \mu_W) \quad Y' \quad H_e/L(\log_e \omega)\ d\mu_W\ d\omega \qquad [11]$$

$$\text{or } R = \int \text{Angle} \int \text{Freq.} \begin{pmatrix}\text{Point Sea}\\ \text{Spectrum}\end{pmatrix} \begin{matrix}\text{Spreading}\\ \text{Function}\end{matrix} \quad (\text{RAO})\ d\begin{pmatrix}\text{wave}\\ \text{angle}\end{pmatrix} \quad d(\text{Freq.})$$

where R = mean square ship response

$= 2 \times \text{variance} = 2 \times \sigma^2$

Or the root-mean-square (r.m.s.) response is,

$$\sqrt{R} = \sqrt{2}\ \sigma$$

$$= \sqrt{2} \times (\text{r.m.s. of record})$$

Therefore, if a record corresponding to the spectrum were available, the r.m.s. value (root-mean-square of equal time-spaced H_e L values) would be,

$$\sigma = \sqrt{R/2}$$

The "r.m.s. of record" is a fundamental statistical quantity associated with the physical phenomenon, and from it "r.m.s. peak-to-trough," generally referred to as $\sqrt{E}$, can be estimated. If the narrow-spectrum assumption can be assumed to apply, $E = 2\sqrt{2}\ \sigma$.

Since ship bending moments are usually quoted as hogging or sagging, then "r.m.s. peak-to-mean" is one-half as great, or r.m.s. H_e/L (hog or sag = $\sqrt{2}\ \sigma$.

In this report, bending moment data for irregular sea conditions are usually plotted in terms of r.m.s. peak-to-mean H_e/L (hog or sag). However, in some cases the r.m.s. of record, σ is used and hence -- in order to avoid confusion -- the lower case h_e/L symbol is then used.

The above relationships between the r.m.s. of the record σ and the r.m.s. peak-to-trough or peak-to-mean are correct, as noted, for narrow-band type of spectrum. Ideally, for this type the above relationship will be correct, i.e.:

$$\sigma = \frac{\sqrt{E}}{2\sqrt{2}} \qquad [12]$$

However, for the other extreme condition representing a very wide frequency spectrum (white noise) the peaks of a record will be best represented by a normal distribution. In this case the relationship will be:

$$\sigma = \frac{\sqrt{E}}{2}$$

It is evident that in reality some intermediate relationship will usually be appropriate, given by:

$$\sigma = \frac{\sqrt{E}}{2\sqrt{2 - \varepsilon^2}} \qquad [13]$$

where ε represents the type of spectrum, with $\varepsilon = 0$ for the narrow and $\varepsilon = 1$ for the wide type. An estimate of ε can be obtained from the ratio of zero crossings to peaks and troughs. It has been found that a ship bending moment spectrum is almost always narrower than the corresponding wave spectrum, and hence it is generally satisfactory to use Equation [12].

The computer printout gives values of "r.m.s. of record," h_e/L, for each of seven headings -- 0°, 30°, 60°, 90°, 120°, 150° and 180° -- and for each of the spectra in each wave group at one speed; e.g., if one significant wave height group is composed of 10 sample spectra then the output of the program would consist of 10 r.m.s. values for the 180° heading, 10 for 150° heading, etc., giving a total of 70 r.m.s. values.

The mean r.m.s. of record and standard deviation of h_e/L values were then calculated for each heading. (The larger the number of spectra available in each group, of course, the better the estimate of standard deviation). Initially the standard deviation, s, was calculated as follows:

$$s = \sqrt{\frac{\sum (X_i - \bar{X})^2}{n}} \qquad [14]$$

However, it is statistically preferable to use

$$s = \sqrt{\frac{\sum (X_i - \bar{X})^2}{n-1}} \qquad [15]$$

where s is the estimator of the standard deviation. It should be noted that if we wish to investigate the confidence interval for standard deviation we use $s^2 = \frac{\sum (X_i - \bar{X})^2}{n}$. The fact that n is used here, rather than n-1 as above, becomes academic because in the investigation the denominator cancels out.

After study of the Wolverine State log data, it was concluded that there was equal likelihood that the ship could be at any heading. Therefore, the overall averages of the means and standard deviations could be calculated by equal weighting of results for all headings, i.e.,

Average mean r.m.s. of record is the arithmetic average of σ for all headings.

Average standard deviation, s, is obtained from (see Appendix B):

$$s_2{}^2 = \frac{1}{n} \sum_{i=1}^{n} (s_i{}^2 + m_i{}^2) - \frac{1}{m} \left\{ \sum_{i=1}^{m} m_i \right\}^2 \qquad [16]$$

where

s_2 = average standard deviation of bending moment in relation to wave height,

s_i = standard deviation of r.m.s. for one heading,

m_i = mean of r.m.s. for one heading,

n = number of headings.

These calculations were also computerized, and the average means and average standard deviations of r.m.s. of record were obtained for each of the wave groups.

Fig. 18 illustrates the results obtained for the Wolverine State in the North Atlantic using the H-family of spectra of Fig. 4. The results are given for the 8- and 16-knot ship speeds in terms of the r.m.s. of record, h_e/L, and standard deviations.

A similar relationship to that given in Fig. 18 for model tests was obtained from full-scale analysis of stress and wave height data based on a typical voyage across the Atlantic (east and westbound), Fig. 8C in Appendix C illustrates the relationship between significant wave height and the r.m.s. of record, h_e/L, for both model and full-scale. Mean and standard deviation are given for both cases. Although the range covered by the full-scale results is limited in terms of the maximum wave height encountered on this particular voyage, the agreement in the range shown is very good. The method used to obtain the full-scale relationship is given in Appendix C.

As previously explained, random samples of sea spectra were not available for the North Pacific ocean. Hence, spectral formulations based on different values of H_V and T_V had to be used. Generally for each of six values of H_V there are six values of T_V and hence six spectra having a known probability of occurrence (instead of random spectra of equal probability). The calculation of mean r.m.s. response and standard deviation then involves the following relationship, applicable within any one band of H_V values:

$$s_2 = \sqrt{\sum (X_i - \bar{X})^2 \; P(T_V)}$$

$$\text{where } P(T_V) = \frac{\text{Percentage occurrence of each } T_V}{\sum \text{Percentage occurrence of all } T_V \text{ values}}$$

As will be discussed later, the California Bear operated over a much wider range of drafts than the Wolverine State, and model basin results showed considerable variation in bending moment with draft. Hence, Fig. 19 gives the California Bear results in terms of h_e/L (r.m.s. of record) for both drafts at which model tests were run, as well as for both speeds.

Results for the California Bear are also given in Fig. 20 in terms of h_e/L, the r.m.s. of record, for one average draft. The results shown here

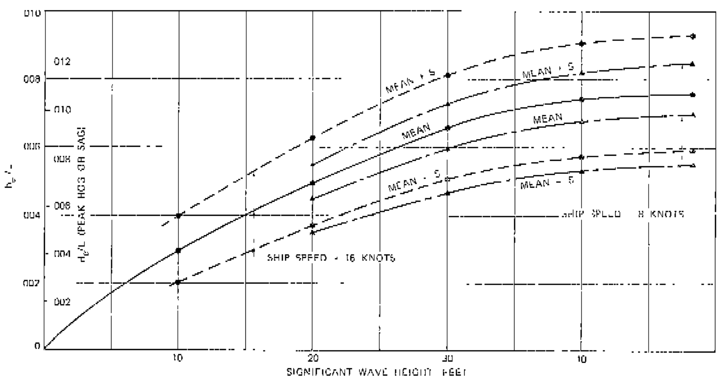

Fig. 18. Predicted Trend of Bending Moment and Standard Deviation for WOLVERINE STATE

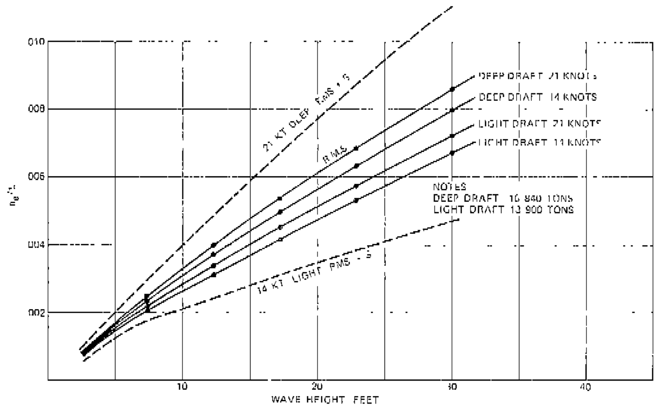

Fig. 19. Predicted Trend of Bending Moment for CALIFORNIA BEAR at Deep and Light Drafts

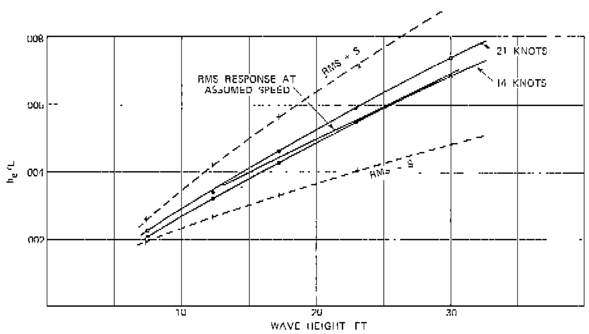

Fig. 20. Predicted Trend of Bending Moment at Average Draft, S.S. CALIFORNIA BEAR (Δ = 14,420 tons)

were interpolated to represent the average full-scale loading condition, Δ = 14,420 tons. (It should be noted that the results are not for the average model loading condition). The curves for the two speeds were blended into one curve on the assumption that the ship speed will be reduced as the wave height increases.

Since it was desired to compare the Wolverine State in the North Atlantic with the California Bear in the North Pacific, it was necessary to obtain a comparison of the two methods previously discussed. This could be done for the North Atlantic, since H_V and T_V data are available from I.S.S.C.(11) and N.P.L.(10) that are similar to those by Yamanouchi (12) in the Pacific. Accordingly, the responses of the Wolverine State were calculated from these data and compared with previous results, as shown in Fig. 18.

Fig. 21 illustrates the results obtained for the Wolverine State in the North Atlantic using the alternative wave data. The H-family results shown in Fig. 18 were redrawn along with results of calculations using data published by the I.S.S.C. giving the frequency of occurrence of T_V in each H_V. The I.S.S.C. spectral formulation was also used. The agreement between the two mean curves is excellent up to a 30-ft. wave height, but there is considerable difference in standard deviation in the higher waves (20-30 ft.). This suggests that using H_V and T_V data exaggerates the standard deviation of bending moment. A further comparison will be given in the next section where predicted values are compared with full-scale results on a Beaufort No. basis.

In the case of the I.S.S.C. data, all values greater than 8 meters or 26.00 ft. wave height (and greater than 15 sec. wave period) are classed in one open-ended band. Although data for the highest band have been plotted at 30 ft., separate calculations prepared from Fig. 5 indicate 32.48 ft. as the mid-point of this band. However, it is clearly an estimate, and the exact value cannot be determined accurately. In order to estimate the erro involved with a wrong choice of upper limit of wave height, a series of cal culations was run using the Wolverine State and the California Bear data in the North Atlantic and North Pacific varying the mean wave height and perio values for the upper-most band. The results showed that the open-ended nat ure of the wave data information can only affect the bending moment curve at the highest wave height and has no effect on the curve up to that point. It will be shown later, under discussion of the long-term curve, that due to the small frequency of occurrence of such wave heights the effect of an error in the upper bound on the long-term prediction is very small.

EXPANSION OF MODEL DATA TO FULL-SCALE

The predicted trends of bending moment vs. wave height are not directly comparable with full-scale data. In order to test model predictions against full-scale data, the trends predicted on the basis of significant wave height must be converted to trends with Beaufort No. The relationships between wind and wave height (Figs. 8 and 9) were discussed in a previous section and can be applied here. The wind-wave relationship originally used for the Wolverine State in the North Atlantic (3) was the Moskowitz-ITTC curve shown in Fig. 9. However, the Yamanouchi curve for the North Pacific is seen to be much lower. It

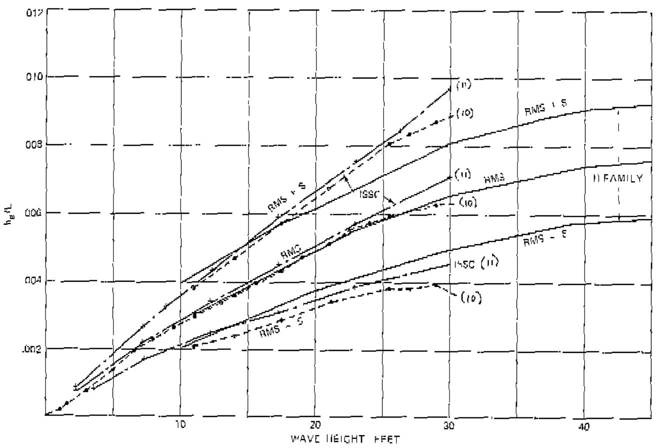

Fig. 21. Comparative Study of Effect of Three Spectrum Formulations in Predicted Bending Trends, S.S. WOLVERINE STATE in North Atlantic

hardly seems reasonable to expect such a large difference to exist between the two oceans. A more reasonable explanation would be that the differences result from differences in the way the data were obtained. Accordingly, Roll's data obtained from visual observations on weather ships (rather than from actual spectra) would appear to be more directly comparable to Yamanouchi's results, obtained by untrained observers.

However, in addition to a general trend of wind vs. wave height it is necessary to know the variability associated with this trend. Hence, standard deviations of wave height were computed from Pierson-Moskowitz wave spectra (9) and the Roll data (18). In the case of Yamanouchi's data, the standard deviation of observed data had already been calculated and plotted (12). See Fig. 10.

Though a rather simple graphical relationship between wave height and wind speed can be used for converting the r.m.s. values from one scale to another, a more sophisticated approach is required to change the standard deviations predicted from model tests on the basis of wave height to the corresponding values on the basis of wind speed, which is essential for the long-term predictions. No matter whether data are classified on the basis of wind velocity or significant wave height, considerable variations from the average wave bending moment or stress can be expected for individual cases in any one weather group. When classified by wind speed, the sea spectra can vary greatly in both shape and area depending on the stage of development of the sea and the presence or absence of swell. On the other hand, classifying by wave height limits the variation to spectrum shape only. It is therefore expected that there will be a larger standard deviation of both wave height and bending moment when classifying on a wind scale basis. This was shown by Compton (25).

The relationship between variance of bending moment on a wind speed basis to that on a wave height basis has been dealt with by E. G. U. Band at Webb Institute, and Appendix A summarizes the preferred approach to this problem. The method is based on the assumption of a uniform linear normal distribution, where the distribution of data is uniform along one axis and normal along the other axis in reference to a mean line. A different approach was also considered whereby it was assumed that the data were normally distributed along both the vertical and horizontal axis about a single mean data point. The first method appears preferable here.

On the basis of the first assumption, Appendix A gives a simple relationship among the variances of the three quantities: wind velocity, wave height (significant) and wave bending moment. The following expression permits the model predictions to be related to wind conditions,

$$S_1{}^2 = \overline{S}_2{}^2 + \tan^2 \theta_2 \left(S_3{}^2 - \frac{\Delta H^2}{12} \right) \qquad [17]$$

where

$S_1{}^2$ = variance of ship response relative to wind as a continuous function (non-dimensional).

$\overline{S}_2{}^2$ = variance of ship response relative to wave height within a weather group (non-dimensional).

$S_3{}^2$ = variance of wave height relative to wind (sq. ft.)

$\tan \theta$ = slope of average curve of ship response (r.m.s. values) vs. significant wave height (1/ft.)

ΔH = increment of width of weather group.

$\overline{S}_2$ is obtained from model data analysis and is plotted in Figs. 18 and 19; S_3 must be obtained from published wave and wind observations. As more data become available from oceanographic studies, the values can perhaps be refined and related to specific ocean areas and seasons.

The standard deviation of bending moment within a weather group is obviously dependent on the range assigned to the group, and the wider the range the greater the standard deviation will be because of changes in the mean value within the range. In the limiting case of infinitesimal widths a continuous function will result. The following relationship between the variance $\overline{S}_2$ within a weather group and the variance S_2 if it is a continuous function is given in Appendix A.

$$\overline{S}_2{}^2 - S_2{}^2 = \tan^2 \theta_2 \, \Delta H^2/12 \qquad [18]$$

This relationship permits one to correct the variance or standard deviation obtained by grouping the data to the value which applies to a continuous function, or vice versa.

Using the above relationships the standard deviations of r.m.s. bending moments were calculated for the Beaufort No. basis, and then were corrected to apply tc a continuous function instead of a series of groups.

The predicted values of r.m.s. bending moment coefficient and standard deviation for both Wolverine State and California Bear are plotted vs. wind speed in Figs. 22, 23 and 24. Some extrapolation was necessary above Beaufort 10, indicating the possible need for more sea spectral data for very severe weather conditions. However, it will be shown later that the effect of different assumptions regarding trends above Beaufort 10 is negligible, since such weather occurs rarely. Table IV illustrates the step by step calculation for the California Bear average draft condition. The increase in the magnitude of standard deviation on the basis of wind speed as compared to that with wave height is substantial.

A summary of the mean and standard deviation of the r.m.s. bending moment coefficient, H_e/L, for the two ships at the appropriate speeds is given in Table V. The means are those obtained for each wave height group assuming equal probability of all headings, while the standard deviation is the corrected value as obtained after conversion to the basis of wind speed rather than wave height. The wind speed is given in the table also.

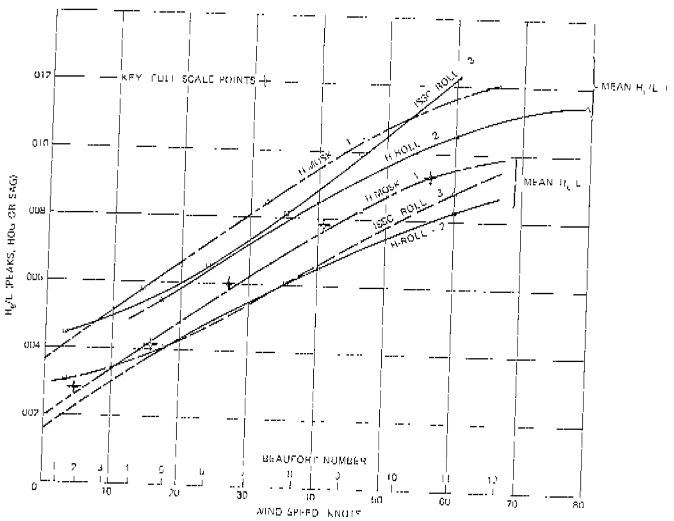

Fig. 22. Predicted and Full-Scale Bending Moment Trends, S.S. WOLVERINE STATE in North Atlantic

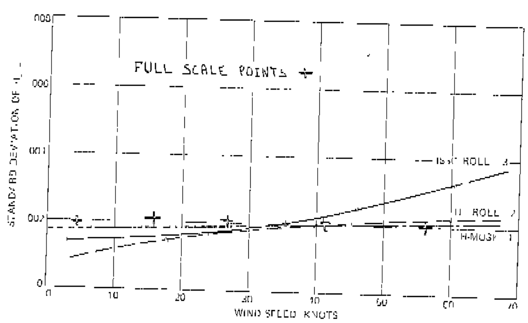

Fig. 23. Predicted Trend of Bending Moment Standard Deviations, S.S. WOLVERINE STATE in North Atlantic

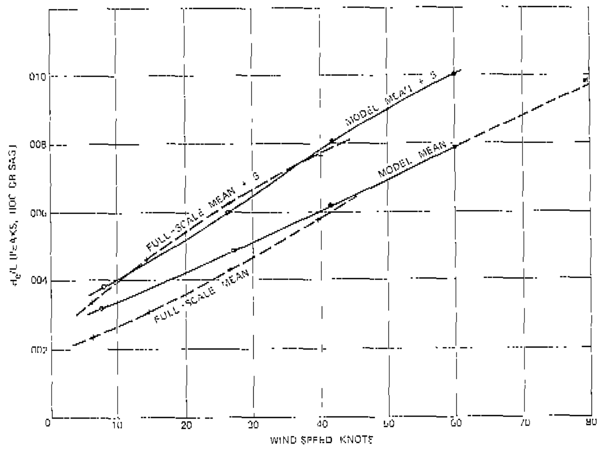

Fig. 24. Predicted and Full-Scale Bending Moment Trends, S.S. CALIFORNIA BEAR in North Pacific

The mean H_e/L and the standard deviation shown in Table V and in Figs. 22, 23, and 24 are given in terms of $\sqrt{E}$, the root-mean-square ship bending moment response, and can be converted to peak-to-trough root-mean-square stress, $\sqrt{E}$, by multiplying by the appropriate factors for each ship as derived in (1).

Examining the curves of Fig. 22 for the <u>Wolverine State</u> in more detail, it will be observed that there are three different model-based predictions using different wind and wave data. Fig. 18 was used as a basis for the calculation in all cases, with speed taken to be 8 or 16 knots, depending on wave height. The different assumptions may be summarized as follows:

Table IV. Sample Conversion of Standard Deviation of H_e/L from Wave Height to Wind Speed Basis

$$S_1^2 = \bar{S}_2^2 + \left[S_3^2 - \frac{\overline{\Delta H}^2}{12} \right] \tan^2 \theta_2$$

THE SAMPLE IS FOR THE <u>CALIFORNIA BEAR</u> IN THE PACIFIC
ALL H_e/L and STD. DEV. values are $\sqrt{E}$ values, i.e., r.m.s. x $\sqrt{2}$

Wave Height, $H_{1/3}$, Feet	Wind Speed, W, Knots	Std. Dev. H_e/L vs $H_{1/3}$ S_2	ΔH Feet	Tan θ 1/ft.	Std. Dev. $H_{1/3}$ vs W S_3, Feet	Std. Dev. H_e/L vs W S_1
	(1)	(2)		(3)	(4)	(5)
7.38	8.1	.000425	4.92	.000359	2.26	.00054
12.30	26.9	.001063	4.92	.000314	4.61	.00124
17.22	42.4	.001620	5.33	.000287	7.15	.00185
22.96	59.6	.002130	6.39	.000280	8.05	.00219

NOTES:

(1) From Fig. 9, Yamanouchi Curve.
(2) From superposition calculations in ISSC spectra, Fig. 20.
(3) Slopes of mean curve, Fig. 20.
(4) From Fig. 10, Yamanouchi Curve.

Table V. Summary of Mean H_e/L and Standard Deviations from Model Tests

All H_e/L and Std. deviations are $\sqrt{R}$ values, i.e., r.m.s. $\times \sqrt{2}$.

Approx. Ship Speed, Knots	Sig. Wave Ht., Feet	Wind Speed (from Roll), Knots	Mean H_e/L	Std. Dev. of H_e/L on Wind Speed
		Wolverine State		
16	7.38	3	.00310	.00244
16	12.30	24	.00478	.00240
12	17.22	35	.00608	.00276
8	22.96	46	.00739	.00316
8	30.00	(60)	.00890	.00382
		***California Bear* @ Avg. Draft from Yamanouchi (12)**		
21	7.38	8	.00321	.00054
20	12.30	27	.00485	.00124
18	17.22	42	.00634	.00183
15	22.96	60	.00790	.00219
14	30.00	(79)	.00978	-

Parentheses indicate extrapolated value.

Case	Spectral Family	Wind-wave Relationship and Standard Deviation
1	Selected from Pierson-Moskowitz (9) (17)	Moskowitz random (17)
2	Selected from Pierson-Moskowitz (9) (17)	Roll, modified (18)
3	ISSC formula (11)	Roll, modified

The first case is essentially the same as that previously published (3) and is believed to be basically sound -- because of the good data available for the North Atlantic. It will be noted that the agreement of both means and standard deviations (Figs. 22 & 23) with full-scale results for Case 1 is excellent.

Case 2 shows that using the Roll wave-wind relationship results in a definite under-estimate of both mean bending moment and standard deviation. However, using the ISSC spectral family (Case 3) -- as would be necessary in the Pacific -- reduces the error of the mean at high wind speeds and increases the standard deviation. It will be shown in the next section how the long-term distributions compare for all of these cases.

Turning to Fig. 24, the procedure used for the *California Bear* in the Pacific is analogous to Case 3 for the *Wolverine State* (ISSC formula and Yamanouchi wind-wave relation). Average data for two model drafts were used, and speed was assumed in accordance with wave height. It is surprising to find that mean and standard deviations of bending moment are estimated with better accuracy here by this method than for the *Wolverine State*.

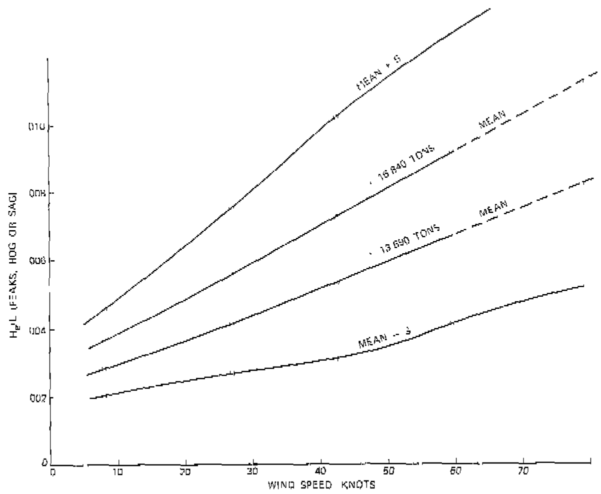

Fig. 25. Predicted Bending Moment Trends at Two Displacements, S.S. CALIFORNIA BEAR, North Pacific

Hence, it can be concluded that the Roll wind vs. wave height relationship for the Wolverine State and the Yamanouchi wind-wave relationship for the California Bear yield reasonable agreement between model and full-scale. Curves such as those in Figs. 22 and 24 were referred to in previous publications (1) as the "limited short-term curves" and are the essential source of information for the derivation, along with the required weather distribution, of the long-term curves.

As indicated earlier, observation of full-scale and model results obtained from the California Bear showed substantial differences in bending moment response between the deep and light draft conditions. Hence, some further consideration of the effect of draft seemed necessary. Fig. 19 illustrates the model results for the deep and light loading conditions at two speeds. From the above four curves two curves were obtained, one for each loading condition at an assumed speed varying in relation to the severity of the sea. Upon conversion to wind speed the two response curves are shown in Fig. 25 in terms of H_e/L vs. wind speed. Similar trends were observed from the full-scale results where the westbound conditions associated with the deep draft, or a displacement of 16,840 tons, and the eastbound conditions (Δ = 12,000) were found to yield substantially different results.

Hence, it was of interest to make model predictions for east and westbound voyages separately. It should be noted that the condition equivalent to the light draft (Δ = 12,000) case could not be reproduced in the model tank due to the model's own weight and the minimum weight condition achieved was equivalent to 13,900 tons displacement. Hence, in order to compare the full-scale eastbound conditions with model tests, a simple linear extrapolation was performed as follows:

$$h_e L\ (\Delta = 12{,}000) = h_e L(\Delta = 13{,}900) - \frac{13{,}900 - 12{,}000}{16{,}840 - 13{,}900}\left[h_e L_{(16{,}840)} - h_e L_{(13{,}900)}\right]$$

The above extrapolation was performed at each Beaufort No. and the results are given in Table VI.

Table VI. h_e/L Bending Moment (x 10^3) RMS and Standard Deviation S.S. CALIFORNIA BEAR

			Δ = 12,000 Extrapolation		Δ = 13,900		Δ = 16,840	
Wave Height, Ft.	Wind Speed, Knots	Ship Speed, Knots	Ave. RMS	Stand. Dev.	Ave. RMS	Stand. Dev.	Ave. RMS	Stand. Dev.
2.46		21.0	.92	.300	1.02	.31	1.17	.37
7.38	8.1	21.0	2.80	.700	3.13	.78	3.64	.91
12.30	26.9	20.1	4.15	1.510	4.71	1.71	5.58	2.00
17.22	42.4	17.8	5.39	2.260	6.14	2.54	7.30	2.97
22.96	59.6	15.3	6.66	2.57	7.62	2.94	9.11	3.54
30.22	79.0	14.0	8.74	3.07	9.45	3.45	11.32	4.13

Fig. 26 shows the model predicted bending moment h_e/L and standard deviation for the westbound and eastbound conditions (Table VI) along with ship results as obtained from full-scale analysis (3). It is evident that the considerable difference between full-scale results for east and westbound voyages is roughly predicted from model tests on the basis of differences in draft.

Comparing the mean curves first it may be seen that model predictions overestimate bending moments somewhat at lower wind speeds both east and westbound -- but especially westbound. Furthermore, the upward trend of the predictions is much less steep than full-scale. However, in the range of 30 - 45 knots the magnitudes are satisfactory. The magnitude of the predicted standard deviations is quite good westbound, but somewhat high eastbound at higher wind speeds. It should, be pointed out, however, that when the mean draft was used as a basis for comparison, as shown in Fig. 24, the agreement between model prediction and full-scale results was much better. The less satisfactory results for east and westbound separately could be due to the reduction in the statistical sample size of the full-scale data as a result of the separation of west and eastbound voyages.

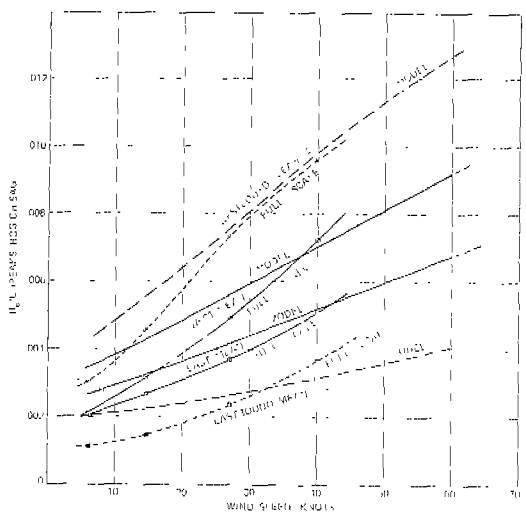

Fig. 26. Predicted Bending Moment Trends, S.S. CALIFORNIA BEAR, North Pacific, Model & Full Scale, East and Westbound Crossings Separated

All in all, one would expect less accurate long-term predictions by the method that had to be used in the Pacific than by the method used in the North Atlantic where better wave data were available.

LONG-TERM PREDICTIONS

We can now determine the long-term distribution of bending moment for any weather group -- and hence for all weathers -- if we make the same two assumptions as in the extrapolation of ship stress data:

1. Actual peak-to-trough values of bending moment over the short-term are Rayleigh distributed.

2. Short-term r.m.s. values for any wave height are normally distributed.

The problem for each weather group then is simply the integration of a large number of hypothetical Rayleigh distributions, each of which is identified and determined by its r.m.s. value, when the r.m.s. values are themselves normally distributed with known standard deviation. The procedure is exactly the same as that used in the extrapolation of full-scale stress data (1)(3) and yields a cumulative distribution for each weather group.

The final step in the prediction is to make a weighted integration of the above curves for individual weather groups on the basis of the frequency of occurrence of the different weather conditions. A computer program was prepared at Webb and used for both model and full-scale data (listings are given in Appendix D), and the results of the predictions are given in Figs. 27 to 29. Fig. 27 shows the long-term curves for the Wolverine State as originally predicted (3) and as recalculated using Roll wind-wave data. It may be seen that simply substituting Roll wind-wave relations (previously referred to as Case 2) leads to a slightly lower trend than the original prediction method (Case 1) which agrees with full-scale results. However, using the ISSC spectra as well (Case 3), with the resulting higher standard deviations, gives a definite overestimate. Hence, it would be expected that the analagous method in the Pacific should yield results that are too high -- hence on the safe side.

Fig. 28 gives California Bear predicted curves separated into east and westbound voyages. Both east and westbound predictions are seen to be overestimated by about the same amount. Fig. 29 gives combined east and westbound results which again show overestimation in comparison with full-scale, although of smaller magnitude. This result is not surprising in view of the overestimate obtained above for the Wolverine State using this same method.

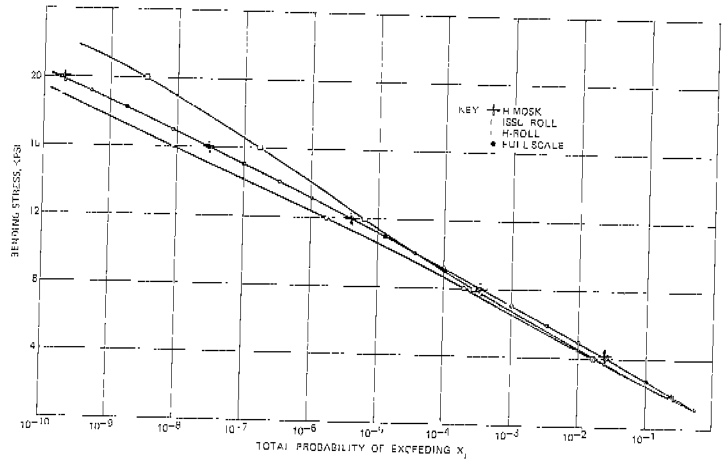

Fig. 27. Long-Term Trends of Bending Moment by Alternate Techniques Compared to Full Scale, S.S. WOLVERINE STATE in North Atlantic

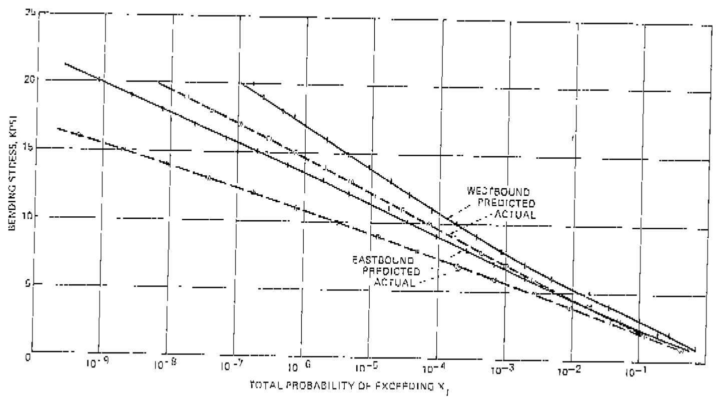

Fig. 28. Long-Term Trends of Bending Moment, S.S. CALIFORNIA BEAR, in Actual Weather, North Pacific

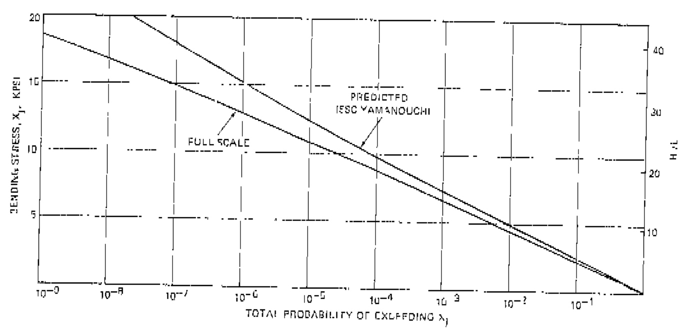

Fig. 29. Long-Term Trends of Bending Moment - Predicted and Full Scale

CONCLUSIONS

As pointed out in other reports (1)(3), a purely statistical treatment of the ship wave bending moment problem cannot yield a satisfactory general design tool. Statistics are helpful in designing similar ships to those for which stress data were collected but cannot provide direct guidance in designing different ships.

The first step toward developing a design tool is described in this report. It is shown that long-term trends of wave bending moment can be predicted from model tests and ocean wave data, using the results of full-scale statistical analysis and extrapolation as a check of predicted trends. For this step to be satisfactorily accomplished, however, it is necessary to have sufficient such full-scale verifications of predicted long-term distributions to give unqualified acceptance of the technique. Furthermore, as pointed out in this report, adequate ocean wave data are needed for all important trade routes.

Another step in design application will be the determination of a probability level to adopt for design wave bending moment. It is necessary first of all to consider the safety of the ship and its crew. The only sound basis for a strength standard in this respect is one based on probability theory. We must be sure that the total risk of structural failure is never greater than society can accept. As progress is made in developing techniques for predicting long-term trends of various loads acting on a ship's hull, along with sophisticated techniques for determining detailed distributions of stresses, the time is approaching when we should decide what risk of structural failure is acceptable to society. Here the classification societies can be of assistance by analyzing their records to determine the number of major failures occurring over the years in ships of different types and sizes and computing the corresponding probabilities that have presumably been considered acceptable (25).

The final step in the practical application of new techniques to ship design will be the rational combining of wave bending moments with other design loads, such as still water bending and dynamic springing or slamming effects at sea.

It has been pointed out elsewhere (3) that a long-term distribution curve of bending moment or stress can also be utilized as a partial definition of anticipated loads for fatigue considerations. However, this interesting possibility does not lie within the scope of this project or this report.

The following specific conclusions can be drawn from the present work:

1. A previously published procedure (3)(4) for predicting long-term distributions of bending moment for a new ship design on the basis of model test data and ocean wave spectra has been extended to cover situations in which ocean wind and wave data are less complete than in the North Atlantic, i.e., available in the form of tabulated wave heights and periods.

2. When the modified technique is applied to the S.S. Wolverine State in the North Atlantic, it is found to overestimate the long-term trend of bending moment, whereas the earlier procedure (using observed wave spectra (8)) agrees very closely with full-scale trends.

3. When the modified technique is applied to the S.S. California Bear in the North Pacific it is found to again overestimate the long-term trend of bending moment. However, it provides a good approximation that is on the safe side.

4. When east and westbound voyages of the California Bear are compared separately, the differences may be accounted for on the basis of draft differences, and trends are further overestimated, perhaps because of an inadequate sample size of full-scale data.

5. In general, it is evident that success in using the prediction discussed is dependent -- at least in part -- on the quality of sea data available. Hence, more complete and accurate ocean wind and wave data are clearly needed, including wave records from which spectra can be determined, particularly for other important trade routes besides the North Atlantic.

6. Meanwhile, it is believed that the application of the procedure for predicting long-term bending moment trends to two different ships in two different oceans has demonstrated a rational basis for the quantitative determination of wave bending moment requirements for possible new designs of the future. This is felt to be the ultimate combined objective of the Ship Structure Committee projects SR 153, SR 165 and SR 171.

In general it appears, therefore, that predictions of long-term trends made on the basis of model tests are satisfactory when adequate ocean wave data in spectral form are available. For design predictions to be made on a routine basis for ships of any size and hull form on any service, the following are required:

(a) Additional wave data in the form of records that can be spectrally analyzed for important trade routes, such as the North Pacific and the area around the Cape of Good Hope.

(b) Additional verification of the prediction procedure by means of further comparisons between predicted and observed long-term trends for ships of various sizes and hull forms.

ACKNOWLEDGMENTS

The authors wish to acknowledge the guidance provided by the Ship Research Committee throughout this project. Numerous members of the Webb research staff, past and present, have made contributions to the work reported here. Professor Robert Zubaly of SUNY Maritime College and Richard van Hooff, Webb Research Associate, assisted in many of the calculations. Otto J. Karst, Professor of Mathematics, E. G. U. Band of Westinghouse Electric Corp., Ocean Research and Engineering Center, and Dr. M. K. Ochi of NSRDC provided valuable consulting assistance in regard to various aspects of probability theory. Mr. Edward Numata of the Davidson Laboratory provided the indispensible model test data, and Teledyne Materials Research provided the full-scale stress data. Appendix C is based on a correlation study carried out under the sponsorship of the American Bureau of Shipping.

Dr. James Williamson, one of the co-authors, who was at Webb Institute of Naval Architecture at the time this report was prepared, is presently Director of Studies, School of Maritime Studies, the Northern Ireland Polytechnic, Jordanstown, North Ireland.

REFERENCES

(1) HOFFMAN, D. and E. V. Lewis, "Analysis and Interpretation of Full Scale Data on Midship Bending Stresses of Dry Cargo Ships," SSC Report 196, June 1969.

(2) HOFFMAN, D., R. van Hooff and E. V. Lewis, "Evaluation of Methods for Extrapolation of Ship Bending Stress Data," Webb Institute report, December, 1970; submitted to the Ship Structure Committee.

(3) LEWIS, E. V., "Predicting Long-Term Distributions of Wave-Induced Bending Moment on Ship Hulls," SNAME Spring Meeting, March 1967.

(4) COMPTON, R. H., "The Prediction of Long-Term Distributions of Wave-Induced Bending Moment from Model Tests." Marine Technology, April 1968.

(5) ST. DENIS, M. and W. J. Pierson, "On the Motions of Ships in Confused Seas," SNAME Transactions, 1953.

(6) LEWIS, E. V., "A Study of Midship Bending Moments in Irregular Head Seas," Journal of Ship Research, Vol. 1, 1957.

(7) LONGUET-HIGGINS, "On the Statistical Distribution of the Heights of Sea Waves," Journal of Marine Research, Yale University, Vol. XI, No. 3, December 31, 1952.

(8) LEWIS, E. V., "The Motion of Ships in Waves," Chapter IX of Principles of Naval Architecture, SNAME, 1967.

(9) MOSKOWITZ, L., W. J. Pierson Jr., and E. Mehr, "Wave Spectra Estimated from Wave Records Obtained by the O.W.S. Weather Explorer and the O.W.S. Weather Reporter," N. Y. U. Report, Part I, November 1962; Part II, March 1963; Part III, June 1965.

(10) HOGBEN, N., F. E. Lumb, and D. E. Cartwright, NPL Ship Report 49, 1964, "The Presentation of Wave Data from Voluntary Observing Ships."

(11) Proceedings of 2nd International Ship Structures Congress, 1964; Report of Committee No. 1.

(12) YAMANOUCHI, Y., S. Unoki and T. Kanda, "On the Winds and Waves of the Northern North Pacific Ocean and South Adjacent Seas of Japan as the Environmental Conditions for the Ship," Ship Research Institute, Tokyo, Japan, March 1965.

(13) PIERSON, W. J. and L. Moskowitz, "A Proposed Spectral Form for Fully Developed Wind Seas Based on the Similarity Theory of S. A. Kitaigorodski," New York University Research Division, Report 68-12, October 1963.

(14) ZUBALY, R. B. and E. V. Lewis, "Ship Bending Moments in Irregular Seas Predicted from Model Tests," Webb Institute of Naval Architecture, 1963.

(15) CANHAM, H. J. S., D. E. Cartwright, G. J. Goodrich and N. Hogben, "Seakeeping Trials on OWS Weather Reporter," RINA Transactions, 1962.

(16) PIERSON, W. J., Jr., Editor, "The Directional Spectrum of a Wind Generated Sea as Determined from Data Obtained by the Stereo Wave Observation Project," Meterological Papers, New York University Report, June 1960.

(17) MOSKOWITZ, L., "Estimates of the Power Spectra for Fully Developed Seas for Wind Speeds of 20 to 40 Knots," Technical Report, N. Y. U. Research Division, 1963.

(18) ROLL, H. U., "Heights, Length and Steepness of Sea Waves in the North Atlantic and Dimensions of Seaways as Functions of Wind Force," SNAME T & R Bulletin No. 1-19 (Translation from German) 1958.

(19) SCOTT, J. R., "Some Average Sea Spectra," Transactions RINA, 1967.

(20) CHIOCCO, M. J. and E. Numata, "Midship Wave Bending Moments in a Model of the Cargo Ship, Wolverine State, Running at Oblique Headings in Regular Waves," SSC report 201, September 1969.

(21) NUMATA, E. and W. F. Yonkers, "Midship Wave Bending Moments in a Model of the Mariner Class Cargo Ship California Bear Running at Oblique Headings in Regular Waves," SSC report 202, November 1969.

(22) SWAAN, W. A., "Amidship Bending Moments for Ship in Waves," International Shipbuilding Progress, Vol. 6, No. 69, August 1959.

(23) MURDEY, D. C., "On the Double Peaks in Wave Bending Moments Response Curves," Trans. RINA, 1969.

(24) COMPTON, R. and R. B. Zubaly, "Further Study of the Use of Model Test Data to Predict Statistical Trends of Wave Bending Moment," Webb Institute of Naval Architecture Report, 1964.

(25) COMPTON, R., "Investigation of Wave-Induced Ship Bending Moments in Typical Sea Spectra," M.S. Thesis, Webb Institute of Naval Architecture, May 1964.

(26) BEER, W. J., "Analysis of World Merchant Ship Losses," Trans. RINA 1969.

APPENDIX A

RELATIONSHIP BETWEEN STANDARD DEVIATION OF HULL RESPONSE WITH RESPECT TO WIND AND WITH RESPECT TO WAVE HEIGHT

by

D. Hoffman

and

E. G. U. Band

INTODUCTION

Problems arise when comparing predictions of ship bending moments made from tests of ship model response in waves with data from full-scale observations classified according to the Beaufort scale (or wind speed). In particular, it is required to convert statistical values such as the standard deviation (S_2) of the rms bending moment at a constant significant wave height, predicted from model tests, to the corresponding full-scale standard deviation (S_1) of rms bending moment at constant wind speed. No direct relation exists between S_1 and S_2. Here the wave height H depends on the wind velocity W, although it shows considerable scatter (i.e. large S_3).

Basic Relationships

The inter-relationships between two- and three- dimensional groups of data can be described in a number of ways. Two of the simplest forms of distribution to treat analytically are described below. A sample calculation based on the second case will be given in some detail, both to show the proposed method for manipulating the data and also to verify the validity of the method.

Case I

In this idealized case, the distribution of ship response in any wind velocity band is assumed to be normal with varying wind velocity. The mean of the distributions is assumed to be a linear function of wind speed, while the standard deviation is invariant. Furthermore the number of data points within any wind speed band is assumed constant, i.e., the distribution along the mean line is uniform. Such a two-dimensional, uniform, linear normal distribution is shown in Fig. 1A for ship bending moment or stress, X, vs. wind velocity, W.

The two standard deviations, S_1 and S_1', are each constant, where

S_1 is the standard deviation of X at constant W, and

S_1' is the standard deviation of W at constant X.

It can be shown that, in this case, S_1 and S_1' are simply related by,

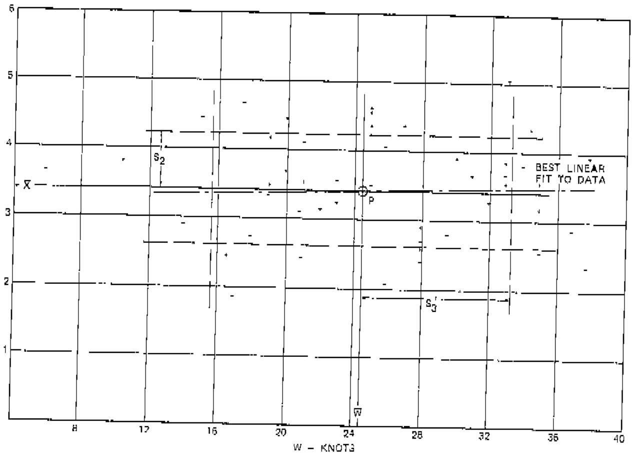

Fig. 3A. Experimental Data Showing Distribution of Bending Stress X with Respect to Wind Speed W for 14 ft. < $H_{1/3}$ < 16 ft.

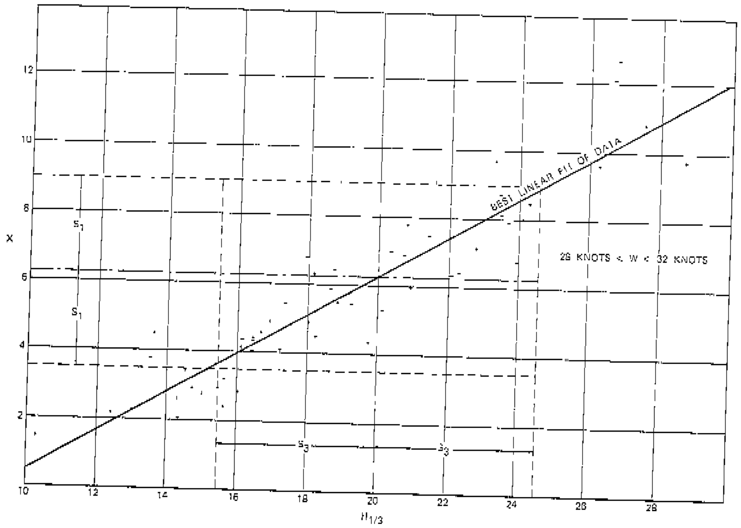

Fig. 4A. Experimental Data, Distribution of Bending Stress X Versus Signif-igant Wave Height, $H_{1/3}$

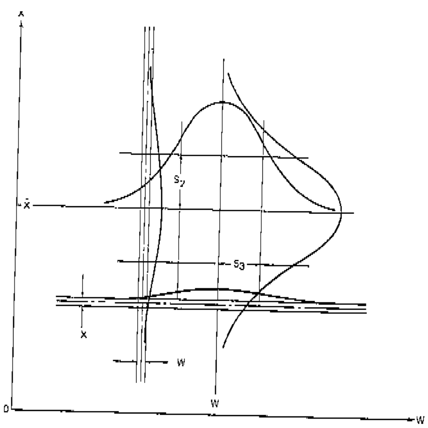

Fig. 5A. "Target Distribution" of X with Respect to W for a Small ΔH

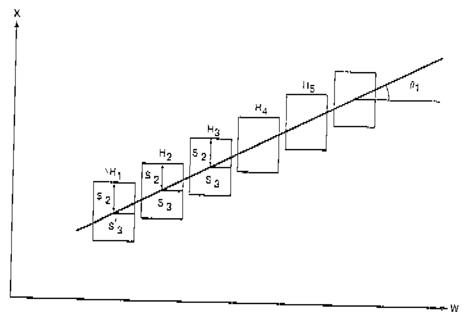

Fig. 6A. Diagram Showing Distribution of X with Respect to W for Discrete Values of ΔH

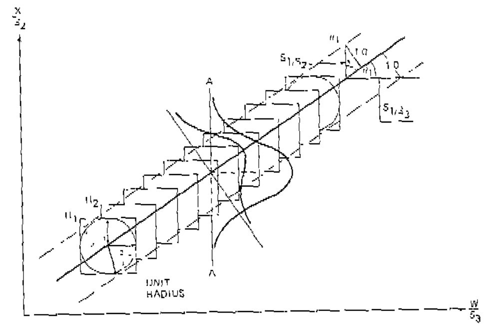

Fig. 7A. Normalized Presentation of Fig. 6A.

squares, and θ_1, changes to θ_1'. (Fig. 7A). It is then possible to sum up the data along a line such as A–A to obtain the contributions of the different overlapping groups of data and to determine the distribution of the total population along A-A. If X and W are independent variables (with H constant), then it can be shown that:

$$S_1 = \frac{S_2}{\text{Cos } \theta_1'} \qquad [3A]$$

$$S_1' = \frac{S_3'}{\text{Sin } \theta_1'} \qquad [4A]$$

and $\tan \theta_1' = (\tan \theta_1) \dfrac{S_3'}{S_2}$ [5A]

A geometrical solution was obtained by Band. See Fig. 7A. Circles are inscribed within the squares and a tangent line drawn above and below the mean line. Then $\frac{S_1}{S_2}$ is the vertical distance from the mean line to either tangent. See Fig. 7A.

The significance of the geometrical solution is that the unit radius of the circle in Fig. 7A represents the standard deviation for cuts through the data at any angle to the axes. Hence, for convenience, one may consider the direction normal to the mean line. Since the standard deviation about the mean line is unity for each portion of the population represented by the individual squares of Fig. 7A, then the standard deviation about the mean line is unity for the entire population. The standard deviation S_1/S_2 of the entire uniformly distributed population, in the direction parallel to the X/S_2 axis, is readily seen to be $\frac{1}{\text{Cos } \theta_1'}$ in Fig. 7A. Thus $S_1 = S_2/\text{Cos } \theta_1$, which is equation [3A].

Similarly Eq. [4A] is derived directly from Fig. 7A,

$$\frac{1}{S_1/S_3'} = S_1 \quad \sin \theta_1$$

Eq. [5] can be obtained from [3A] and [4A] as follows:

$$\sin \theta = \frac{S_3'}{S_1'}$$

$$\cos \theta_1' = \frac{S_2}{S_1}$$

i.e. $\tan \theta_1' = \frac{S_3'}{S_2} \; \frac{S_1}{S_2} = \frac{S_3'}{S_2} \quad \tan \theta_1$

One may now express S_1 in terms of S_2, S_3, θ_2 and θ_3 in the following manner:

$$S_1 = S_2 \; (1 + \tan^2 \theta_1')^{1/2} \qquad \text{from equation [3A]}$$

$$= S_2 \; (1 + (S_3'^2/S_2^2) \;\; \tan^2 \theta_1)^{1/2} \qquad \text{using equation [5A]}$$

$$= (S_2^2 + S_3'^2 \tan^2 \theta_1)^{1/2}$$

$$= \left(S_2^2 + \frac{S_3^2}{\tan^2 \theta_3^2} \quad (\tan^2 \theta_2 \,.\, \tan^2 \theta_3) \right)^{1/2} \quad \text{using eq. [1A] and [2A]}$$

Hence, $S_1 = (S_2^2 + S_3^2 \tan^2 \theta_2)^{1/2}$ [6A]

and similarly

$$S_2 = (S_1^2 - S_3^2 \,.\, \tan^2 \theta_1/\tan^2 \theta_3)^{1/2}$$

$$S_3' = (S_1^2 \,.\, S_2^2)^{1/2} \;\; (\tan \theta_3/\tan \theta_1)$$

Application to Model Stress Data

In many practical examples the available data are grouped into bands of certain width H, and the mean and standard deviation of all points which fall within the band are determined. Generally, the wider the bands the better the continuity of the curve joining the means of the various groups will be (i.e., the easier to fair). However, the standard deviation of data within the groups is not identical to that of a continuous curve. In reality the continuous standard deviation is reduced due to the fact that some of the scatter of data within the bands is eliminated when H tends to zero. (See Fig. 8A).

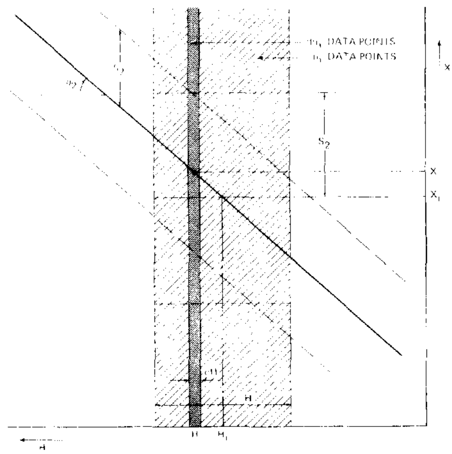

Fig. 8A. Derivation of S_2, the Standard Deviation of the Continuous Line of X vs. H

The above situation exists with the model results as plotted in Figs. 18, 19 and 20 of the main report. The means and the standard deviations are those due to the use of five discrete families of spectra, each representing a band of wave height. Fig. 8A illustrates an enlarged version of part of Figs. 18, 19 and 20 and further analysis is given below.

The mean point of the Δn_i data points that fall in the strip ΔH is at (X_i, H_i), and the standard deviation of these points about X_i is $\bar{S}_2$. The value of $\bar{S}_2$ will depend on the width of the wave height range ΔH. In order that the relationships developed in the previous paragraphs can be applied it is necessary to derive the standard deviation S_2 of the continuous line of X versus H, in terms of ΔH and $\bar{S}_2$.

The data are grouped in increments, ΔH, about a mean data point (H_i, X_i) of Δn_i points.

The standard deviation of each group is $\bar{S}_2$, and it is assumed that ΔH is sufficiently small for the distribution to be treated as uniform over ΔH and for the curve of X vs significant wave height H to be considered as a straight line of gradient $\tan \theta_2$ in the range ΔH. These assumptions are consistent with the uniform linear normal distribution which has been considered above.

The number of data points per unit length $q_i = \dfrac{n_i}{H} = \dfrac{dn_i}{dH}$

where q_i is assumed constant over H. As the second moment of data points about X_i will be equal for both concepts:

$$\Delta n_i \bar{S}_2^{\,2} = \sum_{H_i - \frac{\Delta H}{2}}^{H_i + \frac{\Delta H}{2}} (X - X_i)^2 \, dn_i + \sum_{H - \frac{H}{\Delta 2}}^{H + \frac{\Delta H}{2}} S_2^{\,2} \, dn_i$$

$$q \, \Delta H \bar{S}_2^{\,2} = \int_{H_i - \frac{\Delta H}{2}}^{H_i + \frac{\Delta H}{2}} q_i \tan^2 \theta_2 \, (H - H_i)^2 \, dH + q_i \, S_2^{\,2} \, \Delta H$$

$$\Delta H(\bar{S}_2^{\,2} - S_2^{\,2}) = \tan^2 \theta_2 \frac{\Delta H^3}{12}$$

$$S_2^{\,2} = \bar{S}^2_2 - \tan^2 \theta_2 \frac{\Delta H^2}{12} \qquad [7A]$$

Finally, substituting in the previously derived relationship for S_i, eq. [6A], an expression is obtained for S_i in terms of the experimentally obtained parameters $\bar{S}_2$, θ_2, ΔH, S_3:

$$S_1^{\,2} = \bar{S}_2^{\,2} + \left(S_3^{\,2} - \frac{\Delta H^2}{12}\right) \tan^2 \theta_2 \qquad [8A]$$

This is equivalent to Equation [18] on page 27 of this report.

APPENDIX B

THE DISTRIBUTION OF SEVERAL SUPERPOSED POPULATIONS

by

Dr. Otto J. Karst*

Statement of the Problem

Consider a set of n populations, each described by a density function $f_i(x)$ $(i = 1, 2, \ldots n)$ with known mean μ_i and variance σ_i^2 and having N_i members, respectively, where each N_i is very large. These n populations are combined into one population and the elements thoroughly [illegible] The problem is to find the density function $f(x)$, the mean μ, and the variance σ^2 of the new population in terms of the known density functions, means, variances, and sizes of the original n populations.

We shall assume that each of the constituent density functions [illegible] crete. The results are easily extended to the continuous case.

The Density Function

Assume that each density function is defined over [illegible] X_j $(j = 1, 2, 3, \ldots N_j)$. Define $N = \sum_{i=1}^{n} N_i$ as the total number of elements in the combined population. Then the probability that an element chosen at random from the combined population is also a member of the i^{th} constituent population is $\frac{N_i}{N}$. The probability that this element from the i^{th} constituent population has a particular value of the [illegible] X, say X_j, is then given by $f_i(X_j)$. Hence the probability of [illegible] random variable assuming the value X_j due to a draw of an element from the combined population that is also a member of the i^{th} constituent population [illegible]

$$\frac{N_i}{N} \; f_i(X_j)$$

Hence the total probability that the random variable X can assume the value X_j is

$$\sum_{i=1}^{n} \frac{N_i}{N} \; f_i(X_j)$$

*Professor of Mathematics, Webb Institute of [illegible] since the events in the sum are mutually exclusive.

Therefore the desired density function is given by

$$f(X) = Pr[X = X_j] = \sum_{i=1}^{n} \frac{N_i}{N} f_i(X) \qquad [1B]$$

and $f_i(X)$ is understood to be zero for any $X > N_i$.

We shall now verify that the summation over all X,

$$\sum_{x=1}^{\infty} f(X) = 1$$

We have

$$\sum_{x=1}^{\infty} f(X) = \sum_{x=1}^{\infty} \sum_{i=1}^{n} \frac{N_i}{N} f_i(X)$$

$$= \frac{1}{N} \sum_{x=1}^{\infty} \sum_{i=1}^{n} N_i f_i(X)$$

$$= \frac{1}{N} \sum_{i=1}^{n} N_i \sum_{x=1}^{\infty} f_i(X)$$

But $\sum_{x=1}^{\infty} f_i(X) = 1$ since

$f_i(X)$ is a density function.

$$\sum_{x=1}^{\infty} f(X) = \frac{1}{N} \sum_{i=1}^{n} N_i$$

$$= \frac{1}{N} \cdot N = 1 \qquad \text{Q.E.D.}$$

The mean of the combined population.

By definition: $\mu = E[X]$

$$= \sum_{x=1}^{\infty} x \ f(x)$$

$$= \sum_{x=1}^{\infty} \sum_{i=1}^{n} x \frac{N_i}{N} f_i(x)$$

$$= \frac{1}{N} \sum_{i=1}^{n} N_i \sum_{x=1}^{\infty} x \ f_i(x)$$

But $\sum_{x=1}^{\infty} x \quad f_i(x) = \mu_i$, the mean of the i^{th} constituent population.

Hence,

$$\mu = \frac{1}{N} \sum_{i=1}^{n} N_i \mu_i \qquad [2B]$$

Therefore we see that the desired mean μ is the weighted average of the constituent means, which should come as no great surprise.

The variance of the combined population.

By definition: $\sigma^2 = E[(X - \mu)^2]$, which by a well known procedure reduces to $\sigma^2 = E[X^2] - \mu^2$.

Now,

$$E[X^2] = \sum_{x=1}^{\infty} x^2 \quad f(x)$$

$$= \sum_{x=1}^{\infty} \sum_{i=1}^{n} \frac{x^2 N_i}{N} \quad f_i(x)$$

$$= \frac{1}{N} \sum_{i=1}^{n} N_i \sum_{x=1}^{\infty} x^2 \quad f_i(x)$$

$$= \frac{1}{N} \sum_{i=1}^{n} N_i \mu_{2i}$$ where μ_{2i} = 2nd moment about origin of the i^{th} constituent population.

But

$$\sigma_i^2 = \mu_{2i} - \mu_i^2.$$

Hence

$$E[X^2] = \frac{1}{N} \sum_{i=1}^{n} (N_i \sigma_i^2 + N_i \mu_i^2)$$

$$\sigma^2 = \frac{1}{N} \sum_{i=1}^{n} (N_i \sigma_i^2 + N_i \mu_i^2) - \frac{1}{N^2} \left[\sum_{i=1}^{n} N_i \mu_i \right]^2 \qquad [3B]$$

This formula expresses the variance of the combined population in terms of the statistical parameters μ_i, σ_i, N_i of the constituent populations.

APPENDIX C

CORRELATION OF MEASURED WAVE DATA WITH WIND SPEED AND MEASURED STRESSES

by

Dan Hoffman

Introduction

The analysis at Webb Institute of full-scale stresses recorded on board the Wolverine State (and other ships) on routine commercial service has so far been limited to the method presented in a series of reports (1)(2)(3), in which 20-minute sample records of stress have been put through a probability analyzer by Teledyne Materials Research Company to obtain histograms and/or rms values of peak-to-trough stress. These rms stresses were then plotted against environmental condition in terms of Beaufort No. reported in logbooks. Although some sort of average wave height and average period were also recorded, little credit could be given to these figures because of the inexperience of the constantly changing crew in estimating such quantities visually. Thus the previous analyses were based on two parameters: the wind speed and the rms peak-to-trough value of the 20-minute records.

The installation of the Tucker wave meter on the Wolverine State was intended to alleviate partly the above restriction and to provide some additional information with regard to the environmental conditions, i.e., the significant wave height as well as wind speed. It was expected that some relation could be developed between the measured wave heights and the corresponding wind speeds. Simultaneously, a more refined data reduction could be carried out on some of the wave and stress records by means of spectral analysis, which would lead to precise relationships between stress and wave height. Also, it would make possible a comparison with the stress results obtained from the probability analyzer.

The installation of the Tucker wave meter on the Wolverine State, the reduction of data, and spectral analysis of records were all carried out by the Teledyne Materials Research Company under contract to the Ship Structure Committee (Project SR-153). Additional analysis and interpretation of data at Webb Institute reported herein was in part supported by the American Bureau of Shipping, New York.

Because of several failures of the recorder and a change in routing of the Wolverine State, the analysis of wave records obtained on board was eventually limited to one voyage in the North Atlantic. The particular voyage chosen to be analyzed (No. 277) was found to be the only North Atlantic run for which both valid wave and stress measurements were recorded. It represents a typical trans-Atlantic voyage with roughly 50 single records in both the west and eastbound directions, representing roughly 200 hours in each direction. The weather distribution of the 93 samples is given in Fig. 1C and further illustrated in Table IC. The distribution can be considered to be approximately normal except for truncation at $B_N = 0$. A larger weather distribution based on 1713 records on the Wolverine State taken over 20 voyages in the North Atlantic is also shown in the figure and table, indicating that the comparatively short one-voyage sample agrees quite well with the 20-voyage distribution except above Beaufort 8.

Table IC. Distribution of Weather

B_N*	West	East	Total	Probabilities 1 Voy.	20 Voy.
0	2	5	7	.074	-
1	0	0	0	-	.060
2	2	7	9	.097	.106
3	4	14	18	.194	.192
4	13	6	19	.204	.212
5	12	7	19	.204	.184
6	12	2	14	.151	.096
7	3	1	4	.044	.069
8	3	-	3	.032	.042
9	-	-	-	-	.031
10	-	-	-	-	.006
11	-	-	-	-	.002
	51	42	93	1.000	1.000

*B_N = Beaufort No.

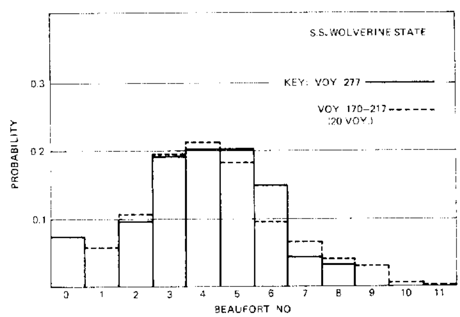

Fig. 1C. Histogram of Weather Distribution as Recorded by S.S. WOLVERINE STATE

The stress distribution with weather (Beaufort No.) for Voyage 277 is given in Fig. 2C, along with the standard deviations. Data for two or more Beaufort Nos. are grouped together. In order to evaluate the adequacy of one voyage in representing a larger sample, the rms mean and standard deviations for 30 voyages were also plotted, as obtained in (1). The agreement of both the means and the standard deviations is exceptionally good, indicating that Voyage 277 can be treated as a sample of the Wolverine State data in the North Atlantic -- at least, up to Beaufort 9.

Analysis of Records

All of the 93 wave records obtained from the Tucker wave meter were spectral analyzed, as well as 45 stress records, 24 westbound and 21 eastbound. Results of spectral analysis of the full-scale records, both wave

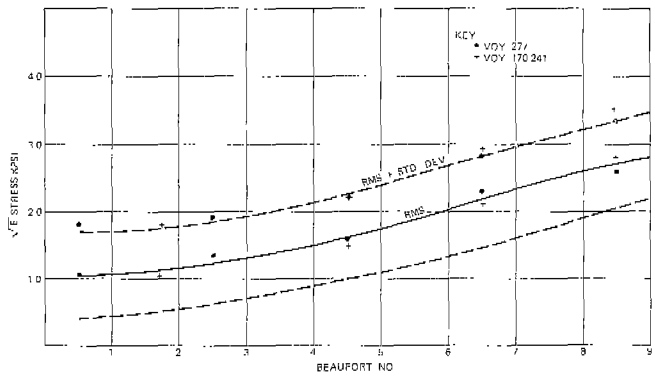

Fig. 2C. Distribution of Short-Term Stress, S.S. WOLVERINE STATE Voyage No. 277

and stress, were supplied by Teledyne in terms of the ordinates of the energy spectrum. For each spectrum a total of 128 such values were given, covering the frequency range of 0 to .5 Hz. In addition, computer graphs in the form of linear and log spectral plots were supplied, along with compressed plots of the wave and stress records themselves.

The data analyzed by Teledyne were originally stored on two reels of 1" 14-channel FM magnetic tape. The data were recorded at 0.3 ips with an FM carrier frequency of 270 Hz for both the data channel and the compensation channel. The data were band-pass filtered before digitization at 24 dB/Octave between .02 - 0.3 Hz. The sampling rate was one sample per second, so that the actual digitization was carried out at 100 times real time with the tape moving at 30 ips. From each record, approximately 30 minutes long, 1024 data points were selected equal to 17 minutes. For each record the spectrum was computed by Teledyne using a digital computer. Each computer printout indicates the number of data points read (usually 1024), as a check on the input parameters, the number of the first data point in the record and the number of raw spectral estimates were averaged to produce the final spectral estimate, which is a chi-squared variable with 32 degrees of freedom. (95% confidence interval is -38%, +44%). Reading in 1024 data points gives 513 raw spectral points, of which only every fourth is sufficient and printed out, resulting in 129 printed points, the first at 0 Hz and the last at 0.5 Hz. The sum of all the spectral ordinates is also given, and to convert it to an approximate integral it must be multiplied by $\Delta f = 0.5/128$, the frequency interval between the printed spectral ordinates. The result is the mean square power of the signal, and its square root, which is given on the printout, is the root mean square (rms) power -- σ_W for wave or σ_S for stress. The scale of the linear spectral plots for most cases was kept constant to allow direct overlaying for comparison.

Data Reduction

Tables IIC and IIIC illustrate the results as obtained from the spectral analysis in terms of the significant wave height and the rms stress. Also shown are results obtained from the probability analyzer for the same west and eastbound voyage. For each record the significant wave height $H_{1/3}$ was obtained as follows:

$$H_{1/3} = 4\sqrt{m_o}$$

where m_o is the area under the wave spectrum curve, $S_\zeta(\omega)$,

i.e., $\sigma^2_W = \int_0^\infty S_\zeta(\omega)d\omega$

where the upper limit of integration is taken at $\omega = 2\pi f = 2 \times 0.5$ [illegible]

$$= 2\pi\Delta f = 2\pi \times 0.5/128$$

The stress was obtained from the spectral analysis as described above, and the rms of the record σ_S was converted to h_e/L. Thus rms bending moment coefficient.

$$h_e/L = \sigma_S \times .0028 \times 1.325$$

where .0028 is the conversion factor from stress to bending moment coefficient as given in (1) and 1.325 is the average calibration factor for port and starboard. Assuming a narrow band spectrum, the rms of record was converted to rms, peak-to-trough, h_e/L, where

$$H_e/L = \sigma_S \times .0028 \times 1.325 \times 2\sqrt{2} = .01483\ \sigma_s$$

Similarly, the $\sqrt{E}$ peak-to-trough rms stress as obtained from the probability analyzer was reduced to a similar form:

$$H_e/L = \sqrt{E} \times .0028 \times 1.325 = .00371\ \sqrt{E}$$

If the assumption of a narrow band spectrum holds, the two values should agree.

The results as tabulated in Tables IIC and IIIC show the actual relationship between the two separately reduced rms values along with the number of zero crossings in the record. These results are plotted and discussed in a later section.

Wind-Wave Height Relationship

The need for a better definition of the environmental condition in studies of ship bending stresses is well demonstrated in Fig. 3C. Three records were chosen to demonstrate the wind-wave relationship, all reported to be of Beaufort scale 5, having the same heading angle and observed wave height and period. The individual wave spectra are given along with the significant wave height calculated from the spectral areas. It is evident that a considerable scatter in significant wave height exists for the same Beaufort condition, H_V and T_V. The results are just as inconsistent on the basis of wind speed. Examination of the log book data indicate an increase in wind up to Record 21 and a decrease from there onward. Record 21 is therefore most likely not a fully developed sea. Record 22 represents the highest significant wave height, although a reduction in wind speed was recorded. It is probably caused by the build-up of the sea during the preceding 12 hours. Record 23 represents the effect of reduction in wind speed over a period of eight hours which causes a reduction in wave height. It is further observed that, except above $\omega = 0.1$, the shapes of the spectra are entirely different in all three cases, representing a double peak, narrow and wide samples. The number of zero crossings in the time record analyzed is shown in Fig. 3C.

The relationship between significant wave height and Beaufort No. was studied for all the cases in hand, and Fig. 4C illustrates the mean relationship and the standard deviation about it. Close to 80% of the total measurements fall within 1 standard deviation. Points corresponding to the mean of Roll's data are also shown for comparison.

It is therefore evident that though the Beaufort No. or wind speed cannot serve as an absolute number in defining the conditions of the sea, it forms a rather powerful statistical estimate so long as the sample is adequately large.

Data showing the relationship between significant wave height and Beaufort No. for east and westbound voyages separately are shown in Figs. 5C and 6C. Somewhat more scatter can be observed than in Fig. 4C.

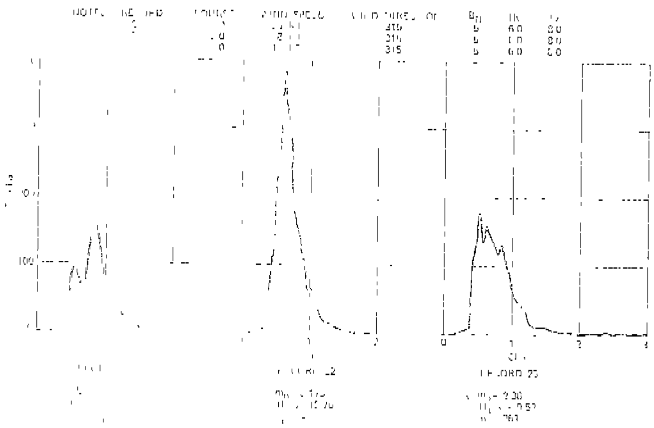

Fig. 3C. Comparative Plot of Three Spectra Recorded, S.S. WOLVERINE STATE in North Atlantic by Tucker Wave Method

Fig. 4C Significant Wave Height Vs. Beaufort Number for East and Westbound Voyages Combined

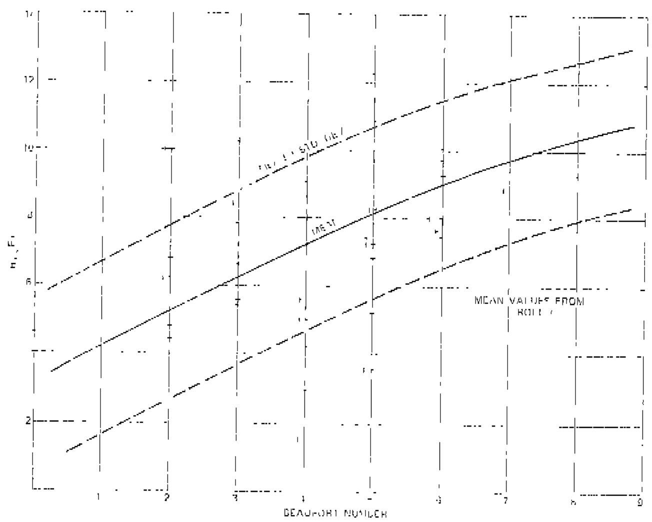

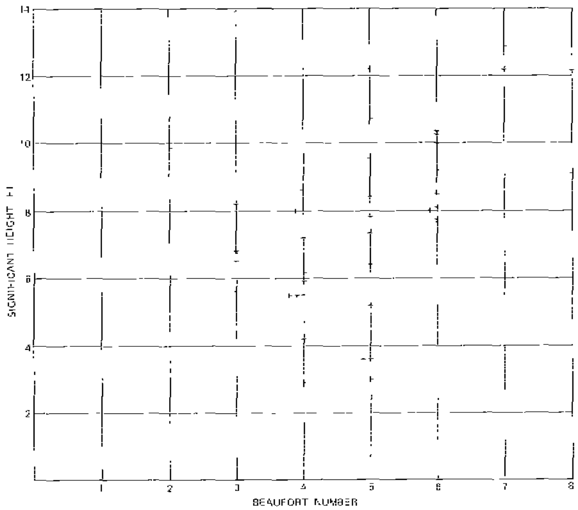

Fig. 5C. Significant Wave Height vs. Beaufort Number for Eastbound Voyages

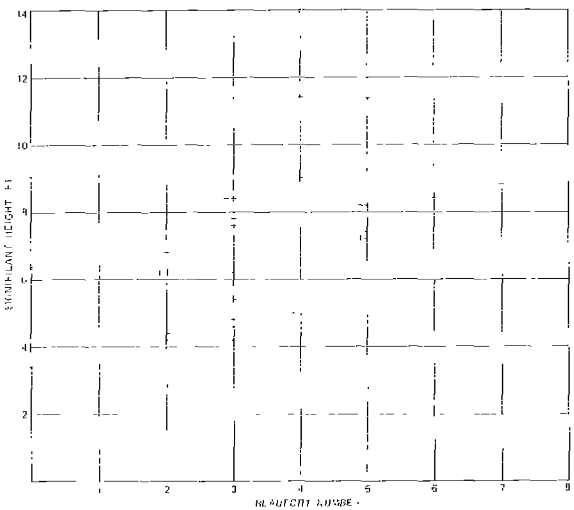

Fig. 6C. Significant Wave Height vs. Beaufort Number for Westbound Voyages

Table IIC. Westbound - H_e/L (Peak to Trough)

Record	$H_e/L \times 10^{-3}$ (P.A.)*	$H_e/L \times 10^{-3}$ (S.A.)*	$H_{1/3}$ (Ft.)
2	3.64	-	4.14
3	4.34	-	5.50
4	5.45	5.69	6.74
5	5.20	5.69	6.50
6	4.60	-	5.59
7	5.35	-	5.94
8	4.97	5.52	6.14
9	5.01	5.47	5.52
10	4.60	4.84	5.54
11	4.66	5.14	5.22
12	8.72	9.88	8.80
13	8.25	9.10	7.96
14	8.94	9.05	7.96
15	8.13	8.85	7.66
16	6.95	-	7.18
17	7.09	7.72	7.76
19	7.90	-	8.46
20	8.16	-	10.34
21	8.50	-	10.75
22	8.90	-	14.08
23	9.95	-	12.20
24	7.86	9.10	10.04
25	7.61	8.26	9.92
26	6.86	7.00	8.20
27	6.98	-	8.60
28	8.06	-	7.94
29	9.16	-	9.96
30	10.18	12.40	12.21
31	10.56	-	9.62
32	8.42	-	8.04
33	8.35	-	7.86
34	7.37	-	7.98
35	6.75	7.66	7.34
36	7.25	7.63	7.38
37	9.06	-	9.20
38	9.58	10.40	9.12
39	11.25	12.46	12.16
40	12.18	13.14	12.90
41	7.16	8.39	7.98
42	8.99	-	10.30
43	6.98	-	9.56
44	4.27	-	6.43
45	4.48	-	3.50
46	1.97	-	2.92
47	0	-	1.59
48	0	-	1.54
49	3.53	4.26	2.95
50	4.16	5.07	3.66
51	5.08	-	3.64
52	0	-	.53
53	0	-	.32

*(P.A.) - Probability analyzer

(S.A.) - Spectrum analysis.

r - no. of cycles in record.

Table IIIC. Eastbound - H_e/L (Peak to Trough) rms vs. $H_{1/3}$

Record	$H_e/L \times 10^{-3}$ (P.A.)	$H_e/L \times 10^{-3}$ (S.A.)	$H_{1/3}$ (Ft.)	n	B_N
55	3.04	3.18	5.36	352	3
56	4.21	4.72	10.16	335	3
57	3.76	-	8.92	299	4
58	3.97	-	8.48	318	3
59	3.67	-	7.68	321	3
60	3.41	-	7.80	359	3
61	3.34	-	4.88	353	3
62	3.41	-	4.44	371	3
63	3.45	3.61	4.70	335	2
64	7.23	-	6.37	121	0
65	5.08	-	6.17	332	2
66	5.04	-	6.16	350	2
67	5.41	-	5.18	343	0
68	4.30	-	4.26	330	2
69	3.19	-	4.93	172	2
70	3.26	-	4.29	303	3
71	3.82	-	3.89	346	4
72	3.34	-	4.56	97	0
73	9.28	10.21	7.54	338	6
74	5.20	7.70	7.16	187	5
1	9.16	9.20	7.17	373	5
2	11.28	12.42	8.88	350	7
3	(13.72)	(13.88)	-	298	9
4	(12.31)	(13.48)	-	295	9
7	6.15	5.95	8.36	357	6
8	4.56	-	5.70	295	0
9	3.49	-	7.19	253	3
10	5.79	8.85	8.72	215	3
11	8.16	6.36	6.26	254	3
12	6.98	7.73	4.63	261	3
13	5.86	5.74	4.44	260	2
14	5.35	6.53	6.82	308	2
17	7.65	-	11.42	247	5
18	8.31	-	9.14	185	3
19	8.43	-	8.38	186	3
20	6.12	7.42	8.20	158	5
21	6.75	7.45	8.20	153	5
22	7.26	-	11.44	136	4
23	11.02	-	7.49	136	5
24	8.05	-	6.76	139	5
25	6.53	5.66	5.06	128	4
26	4.67	5.30	4.94	129	4
27	4.53	4.06	3.92	117	4
28	2.72	3.78	3.30	120	0

Comparison Obtained from Probability Analyzer and Spectral Analysis

The rms stresses, as obtained from a peak-to-trough analysis of the stress records using the probability analyzer, have so far been the only reduced form of stress data available for analysis. Previous reports (1)(2)(3) were based entirely on these rms stresses, and all conclusions derived were on that basis. The spectral analysis, now performed on 42 records, 23 west and 19 eastbound, provide valuable alternative rms data for comparison. Fig. 7C illustrates the relationship between the two sets of stress values, where the 45° line represents the ideal case of equal stress by the two methods. Considerable scatter of data is evident, particularly in the eastbound results. Some of the scatter may simply represent computational error, but the mean line (dashed) through the points shows a significant trend, the spectral values being somewhat higher. Such a tendency can be explained theoretically on the ground that the peak-to-trough stress data do not exactly fit a Rayleigh distribution.

It should be noted that the rms of peak-to-trough stresses was obtained from the spectral analysis by assuming the spectrum was of narrow-band type and the response of the system represents a Gaussian stochastic process. Thus a $\sqrt{2}$ factor was applied to the rms of the record. If a deviation from the above idealized assumption occurs in reality, the factor to be applied is less than $\sqrt{2}$. It is therefore possible that the reason for the average 10- to 15% overestimate from the spectral analysis is due to the fact that the multiplier cannot be bigger than $\sqrt{2}$ and can assume the latter value only under idealized condition. Any deviation from the above will result in a smaller value than $\sqrt{2}$, which on the average for the above tested sample would be $\sqrt{2}$ x .875 = 1.24. Examination of the spectra plots shows in some cases that they are broad, and/or double peaked, which indicates a departure from the narrow band assumption.

Another possible reason for the higher results by spectral analysis may be that the probability analyzer may underestimate the rms peak-to-trough stress because of a slight error in the mean line definition.

Another comparison of the two sets of rms stress data is given in Fig. 8C, where average results are plotted against significant wave height. Results by spectral analysis are shown to be higher over the range of wave heights.

Stress-Wave Height Relationship

A detailed study of the trend of stress as a function of the recorded wave height was made possible for the 42 selected records. Three different sets of stress data were adjusted to a common basis of rms h_e/L bending moment coefficient and plotted in Figs. 8C and 9C in relation to significant wave height:

a) Stress from the spectral analysis.

b) Stress from the probability analyzer peak-to-trough analysis.

c) Stress predicted from model tests in regular waves.

Fig. 9C illustrates the comparison between the rms h_e/L, as obtained from

a) the spectral analysis and from c) model test predictions, in relation to significant wave height. In both cases the standard deviation is also plotted. It may be observed that practically all full-scale observations fall within the limits of the ± standard deviation about the mean obtained from model tests. The relationship between the two mean lines is good particularly in the range of 2 - 10 ft. significant wave height. Above this wave height the lack of full-scale measurements is evident, and the reliability of the full-scale mean line is doubtful.

The good agreement in the range 2 - 10 ft. significant wave height is incidentally an indication of satisfactory accuracy in the Tucker wave meter.

It is also evident again that the results from the eastbound voyage seem to cause most of the scatter. While the model results are based on the assumption of equal probability of each heading, the actual results are biased to certain headings due to the navigational characteristics of a typical North Atlantic crossing. Logbook data for the 42 records show that the headings during eastbound crossing showed wide variations, while headings were consistently quartering seas westbound. This appears to be the reason for greater scatter of h_e/L in the eastbound voyage.

Fig. 10C illustrates a similar relationship between h_e/L values obtained from (b) the probability analyzer and from (c) model test predictions. The model results are reproduced from Fig. 18 of the text. Both

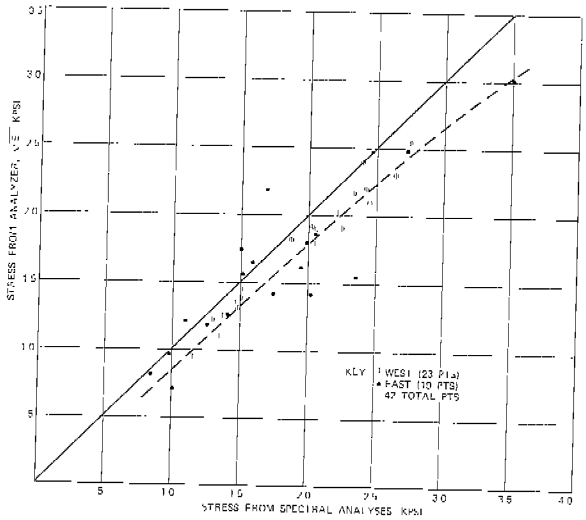

Fig. 7C. Comparison of Stress Data from Spectral Analysis and Probability Analyzer

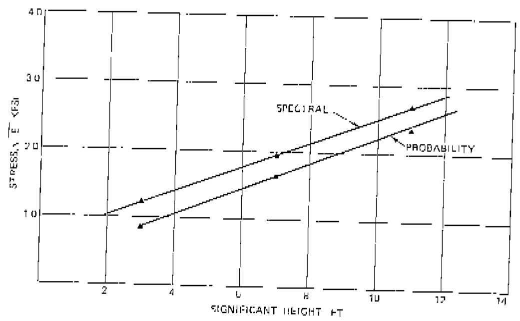

Fig. 8C. Stress Data from Spectral Analysis and Probability Analyzer vs. Significant Wave Height

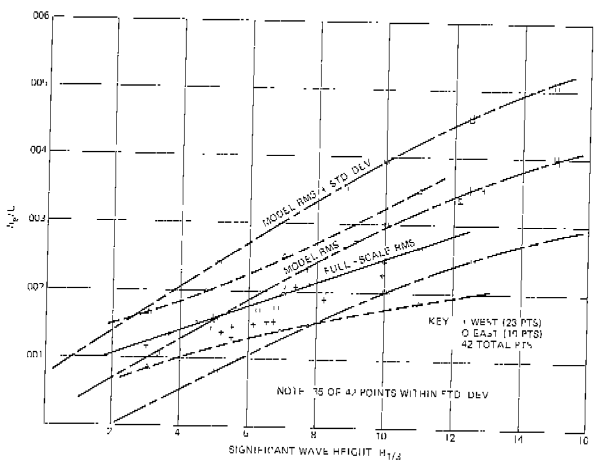

Fig. 9C. Trend of Bending Moment from Spectral Analysis Model Tests

mean lines and their standard deviations are plotted, as well as the individual data points. The general agreement between model and full-scale is not as good as in the previous illustration (Fig. 9C). However, only 13 out of 93 data points (14%) fall outside the ± standard deviation as obtained from model predictions.

It should be noted that Fig. 9C is more consistent than Fig. 10C for comparison purposes, since both model predictions and full-scale analysis yield spectra and the same factor is applied to both to convert to rms h_e/L. But in Fig. 10C the full-scale rms values were determined directly by probability analyzer, as explained previously.

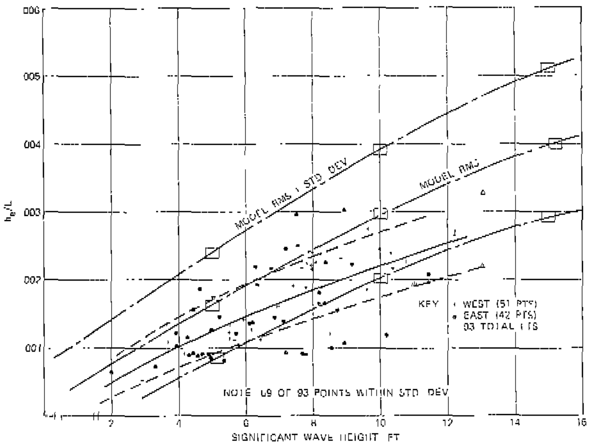

Fig. 10C. Bending Moment from Probability Analyzer & Model Tests vs. Significant Wave Height

Conclusions

The sample voyage of the Wolverine State for which Tucker wave records, as well as stress records, were available for spectral analysis was found to have weather and stress data representative of North Atlantic weather.

Sample wave spectra obtained under the same conditions (Beaufort No.) show wide variations in shape.

The trend of significant wave height against Beaufort No. obtained from spectral analysis of Tucker meter data is in reasonable agreement with Roll as modified by NPL correction factor (9).

The bending moment coefficients obtained by spectral analysis are consistently higher than those obtained by the Sierra probability analyzer. This result may be explained in part by inaccuracy in the probability analyzer. This result may be explained in part by inaccuracy in the probability analyzer and in part by departure of peak-to-trough stresses from a Rayleigh distribution.

Comparison of bending moment coefficients predicted from model tests with the above full-scale alternatives shows better agreement with results obtained by spectrum analysis.

APPENDIX D

COMPUTER PROGRAM

by

D. Hoffman

Description

Program WTS-110 calculates the probability of exceeding a certain stress given the mean and standard deviation of the stresses occurring in each of several weather groups and the probabilities of occurrence of those weather groups.

Theory

The peak-to-trough stresses due to a certain weather condition are assumed to follow a Rayleigh distribution with the RMS values normally distributed within each weather group.

The program finds the probabilities for a series of stresses according to the mean and standard deviation given. Using these stresses as RMS values, it then sums the probability of exceeding a stress level. This is repeated for incremented stresses levels to obtain the general probabilities associated with a series of stress levels in one weather group. For each weather group a weighted addition is made to get the total probability of exceeding each stress.

Usage of the program requires care since the trapezoidal integration can produce large errors under certain conditions.

If the mean value is very low the range of integration will be too low since the integration starts at -1.

Flow Chart for Program WTS110 - Stress Probability for Weather Groups

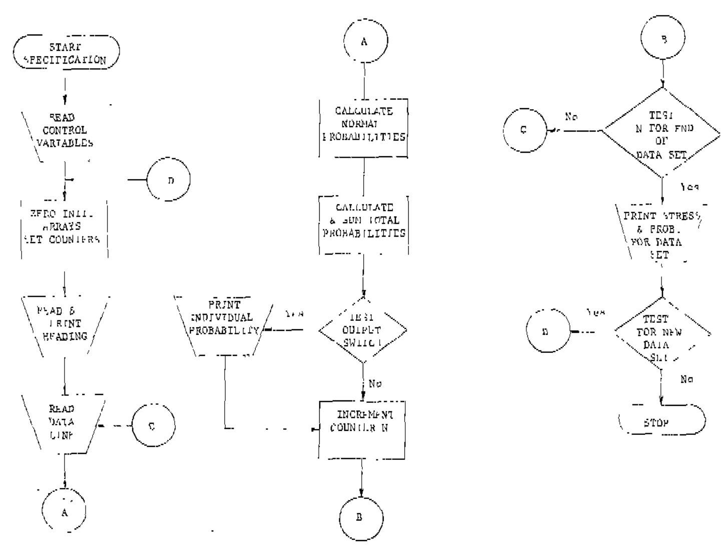

Program Listing

```
WTS110     09:58    RDS2   JUL 06 70 MØN

REAL MEAN
DIMENSIØN RADE(40), PRØB(40),XJ(20),SLW(20),SLB(20)
,GP(20),SX(20)
INTEGER HEAD(50)
CALL ØPENF(1,"WDS110")
READ(1,)K
READ(1,)INC,M,NØ,NU,PINT,CAL
NI=1
200 DØ 20 J=1,M
SLW(J)=0.0
20 SLB(J)=0.0
NI=NI+1
N=1
READ (1,2) (HEAD(J),J=1,50)
2 FØRMAT(50A1)
PRINT 2, (HEAD(J),J=1,50)
300 READ(1,) MEAN,DEV,PW,PB
MEAN=MEAN/CAL
DEV=DEV/CAL
22 DØ 25 I=1,INC
RADE(I)=0.5*(I-1)-0.75
25 PRØB(I)=(.19945/DEV)*EXP(-.5*((RADE(I)-MEAN)/DEV)**2)
105 DØ 120 J=1,M
SX(J)=0.
DØ 110 I=1,INC
XJ(J)=PINT*J
110 SX(J)=SX(J)+PRØB(I)*EXP(-1.0*(XJ(J)/RADE(I))**2)
GP(J)=SX(J)
SLW(J)=SLW(J)+GP(J)*PW
SLB(J)=SLB(J)+GP(J)*PB
120 CØNTINUE
IF (K.EQ.1), GØ TØ 250
PRINT 7,
7 FØRMAT(9X,"XJ",15X,"GP")
PRINT 6,(XJ(J),GP(J),J=1,M)
6 FØRMAT(5X,F8.2,8X,E11.4)
250 N=N+1
IF(N-NU)300,300,140
140 PRINT9,
9FØRMAT(9X,"KPSI",17X,"W.D. 1",17X,"W.D. 2")
PRINT8,(XJ(J),SLW(J),SLB(J), J=1,M)
8FØRMAT(5X,F8.2,15X,E11.4,15X,E11.4)
IF(NI-NØ)200,200,69
69 CALL EXIT
END
```

Description of Input File Contents

Line	Contents
10	K
20	INC, M, NO, NU, PINT, CAL
30	HEAD
40	MEAN, DEV, PW, PB
etc.	(1 line for each Weather Group)
XXX	(NEXT HEADING)
	Data is repeated from Line 30 for each d

Definitions

K	-	OUTPUT SWITCH - ≠1 for Complete Output =1 for Total Probabilities only.
INC	-	No. of Intervals for normal Dist. (Max. 40)
M	-	No. of Stresses (Max. = 20)
NO	-	No. of Data Sets
NU	-	No. of Weather Groups per Data Set
PINT	-	Interval between Stresses
CAL	-	Calibration constant
HEAD	-	Heading for Data Set (Max. 50 CHAR.)
MEAN	-	Mean Stress (μ)
DEV	-	Deviation (σ)
PW	-	Observed Probability for Weather Group
PB	-	Theoretical Probability for Weather Group

Total No. of lines equal ((*No. of weather groups per data set* one) times No. of data sets) Plus 3.

OR

Total = NO(NU + 1) + 3

Sample Input File

```
WDS110     09:36    RDS2   JUL 08 70 WED

10)  5
20)  40,20,1,4,1.0,.0022
30)  CALIFORNIA BEAR EAST - ACTUAL WEATHER
40)  .15262,.40470,.5186,.5
50)  .05534,.00131,.2862,.3
60)  .05416,.04151,.1375,.2
70)  .04539,.30218,.4576,0.0
```

Sample Output

```
WTS110     14:38    RDS2   JUL 06 70 MON
```

CALIFORNIA BEAR EAST - ACTUAL WEATHER

(Stress Level, KPSI) — (Probability of Exceeding Stress in Weather Group)

(First Weather Group)

XJ	GP
1.00	0.4640E+00
2.00	0.8521E-01
3.00	0.9445E-02
4.00	0.8475E-03
5.00	0.5600E-04
6.00	0.3093E-05
7.00	0.1750E-06
8.00	0.8884E-08
9.00	0.3632E-09
10.00	0.1347E-10
11.00	0.5392E-12
12.00	0.2230E-13
13.00	0.8202E-15
14.00	0.2572E-16
15.00	0.7434E-18
16.00	0.2273E-19
17.00	0.7651E-21
18.00	0.2557E-22
19.00	0.7716E-24
20.00	0.2059E-25

(Second Weather Group)

XJ	GP
1.00	0.5980E+00
2.00	0.1946E+00
3.00	0.4577E-01
4.00	0.8753E-02
5.00	0.1452E-02
6.00	0.2161E-03
7.00	0.2941E-04
8.00	0.3761E-05
9.00	0.4539E-06
10.00	0.5175E-07
11.00	0.5680E-08
12.00	0.6053E-09
13.00	0.6221E-10
14.00	0.6161E-11
15.00	0.5953E-12
16.00	0.5666E-13
17.00	0.5294E-14
18.00	0.4816E-15
19.00	0.4271E-16
20.00	0.3731E-17

2.00	0.3192E+00
3.00	0.1207E+00
4.00	0.4001E-01
5.00	0.1207E-01
6.00	0.3392E-02
7.00	0.9610E-03
8.00	0.2287E-03
9.00	0.5587E-04
10.00	0.1321E-04
11.00	0.3039E-05
12.00	0.6816E-06
13.00	0.1496E-06
14.00	0.3221E-07
15.00	0.6816E-08
16.00	0.1419E-08
17.00	0.2913E-09
18.00	0.5903E-10
19.00	0.1184E-10
20.00	0.2336E-11

XJ	GP
1.00	0.7680E+00
2.00	0.4627E+00
3.00	0.2433E+00
4.00	0.1169E+00
5.00	0.5265E-01
6.00	0.2256E-01
7.00	0.9289E-02
8.00	0.3703E-02
9.00	0.1436E-02
10.00	0.5442E-03
11.00	0.2021E-03
12.00	0.7370E-04
13.00	0.2646E-04
14.00	0.9363E-05
15.00	0.3274E-05
16.00	0.1131E-05
17.00	0.3867E-06
18.00	0.1309E-06
19.00	0.4393E-07
20.00	0.1462E-07

(Above output is displayed only if $\alpha \neq 1$. Below output always displayed).

Stress Level, KPSI — Total Probabilities for Given Weather Distributions

KPSI	W.D. 1	W.D. 2
1.00	0.5503E+00	0.5486E+00
2.00	0.1724E+00	0.1648E+00
3.00	0.4862E-01	0.4260E-01
4.00	0.1513E-01	0.1115E-01
5.00	0.5137E-02	0.2878E-02
6.00	0.1829E-02	0.7447E-03
7.00	0.6675E-03	0.1991E-03
8.00	0.2453E-03	0.4687E-04
9.00	0.9054E-04	0.113[illegible]E-04
10.00	0.3313E-04	0.265[illegible]E-05
11.00	0.1225E-04	0.6093E-06
12.00	0.4239E-05	0.1365E-06
13.00	0.1545E-05	0.299[illegible]
14.00	0.5448E-06	0.6445E-0[illegible]
15.00	0.1795E-06	[illegible]
16.00	0.6536E-07	[illegible]
17.00	0.2232E-07	[illegible]
18.00	0.7559E-08	0.11[illegible]
19.00	0.2532E-08	[illegible]
20.00	[illegible]	0.467[illegible]E-12

```
USED: CPU     9.4   I/O     19.4
```

UNCLASSIFIED
Security Classification

DOCUMENT CONTROL DATA - R & D

(Security classification of title, body of abstract and indexing annotation must be entered when the overall report is classified)

1. ORIGINATING ACTIVITY (Corporate author) Webb Institute of Naval Architecture, Glen Cove, New York	2a. REPORT SECURITY CLASSIFICATION Unclassified
	2b. GROUP

3. REPORT TITLE
Correlation of Model and Full-Scale Results in Predicting Wave Bending Moment Trends

4. DESCRIPTIVE NOTES (Type of report and inclusive dates)

5. AUTHOR(S) (First name, middle initial, last name)
D. Hoffman, J. Williamson, and E. V. Lewis
With Appendices by: O. J. Karst and E. G. U. Band

6. REPORT DATE July 1972	7a. TOTAL NO. OF PAGES 62	7b. NO. OF REFS 26
8a. CONTRACT OR GRANT NO. N00024-68-C-5282	9a. ORIGINATOR'S REPORT NUMBER(S)	
b. PROJECT NO.		
c.	9b. OTHER REPORT NO(S) (Any other numbers that may be assigned this report) SSC-233	
d.		

10. DISTRIBUTION STATEMENT
Unlimited

11. SUPPLEMENTARY NOTES	12. SPONSORING MILITARY ACTIVITY Naval Ship Systems Command

13. ABSTRACT Comparison is made between model and full-scale predictions of long-term wave-induced bending moment trends for two ships, the S.S. WOLVERINE STATE and the S.S. CALIFORNIA BEAR.

For predicting such statistical trends of wave bending moment from model tests two basic types of required data are discussed:

a. Wave data from different levels of sea severity, along with relationships between wave heights and wind speeds.

b. Model response amplitude operators as a function of ship loading condition, speed and heading.

Available wave data in different ocean areas are first reviewed. The determination of the wave bending moment responses, and the expansion to full-scale are then shown and discussed.

Comparison of predicted long-term trends with extrapolated full-scale results shows good agreement for the WOLVERINE STATE in the North Atlantic and fair results for the CALIFORNIA BEAR in the North Pacific. The inferiority of the latter is probably due to less refined definition of the sea in this ocean area.

It is concluded that success in using the prediction method presented is a function of the quality of sea data available for the particular service in question.

DD FORM 1 NOV 65 1473 (PAGE 1)

S/N 0101-807-6801

UNCLASSIFIED
Security Classification

14 KEY WORDS	LINK A		LINK B		LINK C	
	ROLE	WT	ROLE	WT	ROLE	WT
Bending Moments						
Stresses on Ship Hulls						
Model Tests						
Full Scale Load Predictions						
Wave Data						

☆U.S. GOVERNMENT PRINTING OFFICE: 1972 724-412/102 1-3

SHIP RESEARCH COMMITTEE
Maritime Transportation Research Board
National Academy of Sciences-National Research Council

The Ship Research Committee has technical cognizance of the inter-agency Ship Structure Committee's research program:

PROF. R. A. YAGLE, Chairman, *Prof. of Naval Architecture, University of Michigan*

DR. H. N. ABRAMSON, *Director, Dept. of Mechanical Sciences, Southwest Research Inst*

MR. W. H. BUCKLEY, *Coordinator of Hydrofoil Struc. Res., Naval Ship R & D Center*

MR. E. L. CRISCUOLO, *Senior Non-destructive Testing Spec., Naval Ordnance Lab.*

DR. W. D. DOTY, *Research Consultant, U. S. Steel Corporation*

PROF. J. E. GOLDBERG, *School of Civil Engineering, Purdue University*

PROF. W. J. HALL, *Prof. of Civil Engineering, University of Illinois*

MR. J. E. HERZ, *Chief Structural Design Engineer, Sun Shipbuilding & Dry Dock Co.*

MR. G. E. KAMPSCHAEFER, JR., *Manager, Application Engineering, ARMCO Steel Corp.*

MR. R. C. STRASSER, *Director of Research, Newport News Shipbuilding & Dry Dock Co.*

CAPT. R. M. WHITE, USCG, *Chief, Applied Engineering Section, U.S. Coast Guard Academy*

MR. R. W. RUMKE, *Executive Secretary, Ship Research Committee*

This project was coordinated under the guidance of the following Advisory Group I, "Ship Response and Load Criteria" membership:

DR. H. N. ABRAMSON, Chairman, *Director, Dept. of Mech. Sciences, Southwest Res. Inst.*

MR. W. H. BUCKLEY, *Coordinator of Hydrofoil Struc. Res., Naval Ship R & D Center*

PROF. A. M. FREUDENTHAL, *College of Engineering, George Washington University*

MR. R. G. KLINE, *Associate Research Consultant, U. S. Steel Corporation*

DR. M. K. OCHI, *Research Scientist, Naval Ship R & D Center*

MR. R. C. STRASSER, *Director of Research, Newport News Shipbuilding & Dry Dock Co.*

CAPT. R. M. WHITE, USCG, *Chief, Applied Engineering Section, U. S. Coast Guard Academy*

SHIP STRUCTURE COMMITTEE PUBLICATIONS

These documents are distributed by the National Technical Information Service, Springfield, Va. 22151. These documents have been announced in the Clearinghouse Journal U.S. Government Research & Development Reports (USGRDR) under the indicated AD numbers.

SSC-220, *A Limited Survey of Ship Structural Damage* by S. Hawkins, G. H. Levine, and R. Taggart. 1971. AD 733085.

SSC-221, *Response of the Delta Test to Specimen Variables* by L. J. McGeady. 1971. AD 733086.

SSC-222, *Catamarans - Technological Limits to Size and Appraisal of Structural Design Information and Procedures* by N. M. Maniar and W. P. Chiang. 1971. AD 733844.

SSC-223, *Compressive Strength of Ship Hull Girders - Part II - Stiffened Plates* by H. Becker, A. Colao, R. Goldman, and J. Pozerycki. 1971. AD 733811.

SSC-224, *Feasibility Study of Glass Reinforced Plastic Cargo Ship* by R. J. Scott and J. H. Sommella. 1971. AD 735113.

SSC-225, *Structural Analysis of Longitudinally Framed Ships* by R. Nielson, P. Y. Chang, and L. C. Deschamps. 1972.

SSC-226, *Tanker Longitudinal Strength Analysis - User's Manual and Computer Program* by R. Nielson, P. Y. Chang, and L. C. Deschamps. 1972.

SSC-227, *Tanker Transverse Strength Analysis - User's Manual* by R. Nielson, P. Y. Chang, and L. C. Deschamps. 1972.

SSC-228, *Tanker Transverse Strength Analysis - Programmer's Manual* by R. Nielson, P. Y. Chang, and L. C. Deschamps. 1972.

SSC-229, *Evaluation and Verification of Computer Calculations of Wave-Induced Ship Structural Loads* by P. Kaplan and A. I. Raff. 1972.

SSC-230, *Program SCORES -- Ship Structural Response in Waves* by A. I. Raff. 1972.

SSC-231, *Further Studies of Computer Simulation of Slamming and Other Wave-Induced Vibratory Structural Loadings on Ships in Waves* by P. Kaplan and T. P. Sargent. 1972.

SSC-232, *Study of the Factors Which Affect the Adequacy of High-Strength, Low-Alloy Steel Weldments for Cargo Ship Hulls* by E. B. Norris, A. G. Pickett, and R. D. Wylie. 1972.